Role of Na^+–K^+-ATPase in the relaxation of rat isolated mesenteric arteries to potassium: dependence on extracellular sodium concentration

D.X.P. Brochet, J.M. Hinton and P.D. Langton

Department of Physiology, School of Medical Sciences, University of Bristol, Bristol BS8 1TD, UK

In 1998, Edwards *et al.* proposed that potassium (K^+) ions could be an endothelial-derived hyperpolarising factor (EDHF); however, the identity of EDHF remains controversial. Subsequent experiments in our laboratory have demonstrated that relaxation to K^+ is not dependent on the presence of an intact endothelium and is ouabain sensitive (Brochet & Langton, 2001), indicating that smooth muscle Na^+–K^+-ATPase may be responsible for K^+-induced relaxations. In the present study we have further investigated the effect of an increase of extracellular concentration of potassium ($[K^+]_o$) on the tone of rat isolated mesenteric arteries.

Male Wistar rats (200–250 g) were stunned and killed by cervical dislocation; third-order mesenteric arteries were dissected free and isometrically mounted for measurement of force. Arteries were contracted with phenylephrine (0.5–2 μM) to 70 % of the maximal response and relaxations measured against this contraction in the presence of *N*-nitro-L-arginine methyl ester (100 μM) and indomethacin (2.8 μM), inhibitors of NO synthase and cyclo-oxygenase, respectively. Raising $[K^+]_o$ from 5.9 to 11.2 mM did not evoke relaxation of arteries with (+E, 106.7 ± 6.3 %; mean ± S.E.M., $n = 7$), or without, an endothelium (−E, 140.6 ± 7.7 %, $n = 5$). When $[K^+]_o$ was initially lowered from 5.9 to 1.2 mM, restoring $[K^+]_o$ back to 5.9 mM produced a relaxation (+E: 17.8 ± 4.2 %, $n = 10$). After lowering $[K^+]_o$ from 5.9 to 1.2 mM for 3 min, increasing $[K^+]_o$ to between 11.2 and 41.2 mM produced a transient relaxation, although concentrations higher than 41.2 mM evoked arterial contraction. Raising $[K^+]_o$ from a range of concentrations, between 1.2 and 5.9 mM, to 13.8 mM resulted in a relaxation that was dependent on the initial $[K^+]_o$. These relaxations were abolished by 100 μM ouabain.

Arterial relaxations following lowered potassium may reflect a build-up of intracellular sodium during reduction of $[K^+]_o$ and the subsequent over-run of the electrogenic Na^+–K^+-ATPase pumping when extracellular potassium is restored. Preventing an intracellular rise of sodium by replacing extracellular sodium with choline or TRIZMA abolished the relaxation to a rise in $[K^+]_o$ from 1.2 to 13.8 mM ($n = 12$ and $n = 6$, respectively).

In summary, these data demonstrate that potassium-induced relaxation involves a ouabain-sensitive mechanism dependent on external sodium concentration, but independent of the endothelium.

Brochet, D.X.P. & Langton, P.D. (2001). *J. Physiol.* **536.P**, 96*P*.

Edwards, G. *et al.* (1998). *Nature* **396**, 269–272.

All procedures accord with current UK legislation.

5-HT activates a non-capacitative calcium channel in small intrapulmonary artery

C. Guibert, R. Marthan and J.-P. Savineau

EMI INSERM (9937), Laboratoire de Physiologie Cellulaire Respiratoire, Université Bordeaux 2, France

Local and circulating concentrations of serotonin (5-HT) increase in response to pulmonary hypoxia and may contribute to pulmonary hypertension (MacLean *et al.* 2000). Under normoxic conditions, 5-HT induces a pulmonary vasoconstriction but there is little information on the 5-HT-induced calcium signal in small intrapulmonary arteries (IPA), which play a central role in blood flow regulation in the lung. We, therefore, investigated the effects of 5-HT on the calcium concentration ($[Ca^{2+}]_i$) in isolated small IPA from rat. Rats were humanely killed according to the national guidelines. IPA with an external diameter of 228.6 ± 8.5 μm ($n = 22$) were isolated by dissection from the left lung. The vessels were loaded with the calcium-sensitive fluorescent dye fura-PE3 (2 μM) for 1.5 h at 37 °C. Digital imaging was used to record $[Ca^{2+}]_i$. Vessels were pressurized at 10 mmHg and the experiments were performed at 37 °C. Significance was tested with Student's paired *t* test ($P < 0.05$). Data are expressed as the means ± S.E.M.

Bath application of 5-HT induced a concentration-dependent intracellular calcium increase with a maximum and a half-maximum effect occurring at 10 and 2.1 μM, respectively ($n = 6$). This 5-HT-induced sustained calcium signal was not significantly modified by L-type calcium channel antagonists nitrendipine (1 μM, $P = 0.13$, $n = 4$) or nicardipine (1 μM, $P = 0.45$, $n = 5$). Depletion of the intracellular calcium store by pretreatment with a sarcoplasmic reticulum Ca^{2+}-ATPase inhibitor (cyclopiazonic acid, CPA, 10 μM) did not affect the calcium response to 5-HT ($n = 6$). Store-operated calcium channel antagonists (LOE 908, SKF 96365 and gadolinium 10 μM, $n = 6$, 7 and 5, respectively) did not modify the 5-HT-induced calcium signal. CPA alone activated a capacitative-like channel sensitive to LOE 908 (inhibition of 71 %, $n = 4$) and insensitive to SKF 96365 ($n = 4$) and gadolinium ($n = 5$), suggesting that 5-HT activates a non-capacitative calcium channel. On the other hand, inhibitors of arachidonic acid production such as a DAG lipase inhibitor, RHC 80267, 50 μM or a G-protein-coupled phospholipase A2 antagonist, isotetrandrine, 10 μM, partially blocked the 5-HT-induced calcium increase by 58 % ($n = 6$) and 51 % ($n = 5$), respectively. Arachidonic acid 100 μM induced a small calcium increase in two out of five vessels, suggesting a synergic mechanism is involved in the calcium response to 5-HT.

Although a capacitative-like calcium influx appears to be present in IPA, the calcium response to 5-HT depends on the activation of a non-capacitative calcium channel. The activation of this channel may partly involve the production of arachidonic acid.

MacLean, M.R. *et al.* (2000). *Br. J. Pharmacol.* **131**, 161–168.

This work was funded by INSERM and Conseil Regional d'Aquitaine.

All procedures accord with current National guidelines.

Changes in Ca^{2+} entry mechanisms following retinoic acid-induced differentiation of neuroblastoma cells

Anna M. Brown, Fiona C. Riddoch, Christopher P.F. Redfern* and Timothy R. Cheek

*Department of Physiological Sciences and *Department of Endocrinology, The Medical School, Framlington Place, University of Newcastle, Newcastle NE2 4HH, UK*

Neuroblastoma cells undergo differentiation in response to retinoids (Redfern *et al.* 1995) and this is the basis of retinoid-based chemotherapy regimes currently in clinical trials for treatment of Neuroblastoma disease. However, not all cells respond to treatment and little is known about the mechanisms underlying this heterogeneity. Since changes in the concentration of intracellular calcium ions ($[Ca^{2+}]_i$) have been hypothesised to be involved in the differentiation of neuroblastoma cells (Celli *et al.* 1999), we are investigating whether changes in Ca^{2+} signalling mechanisms occur following differentiation of SH-SY5Y cells with 9-*cis* retinoic acid (9cRA).

In order to investigate changes in putative Ca^{2+} entry mechanisms we have used fura-2 fluorescence measurements to monitor both changes in $[Ca^{2+}]_i$ and divalent cation entry (Mn^{2+} quench). Fluorescence from fura-2 AM-loaded cells was continuously monitored using a Perkin-Elmer LS-50B fluorimeter with excitation and emission wavelengths of 340 and 510 nm, respectively, for monitoring changes in $[Ca^{2+}]_i$, and 360 and 510 nm for Mn^{2+} quench (Bennett *et al.* 1998).

In the presence of extracellular Ca^{2+} the muscarinic agonist methacholine stimulated a rise in $[Ca^{2+}]_i$ in both control and differentiated cells. The EC_{50} values were similar, 6.8 and 7.1 μM methacholine in control and differentiated cells respectively. However, in the absence of extracellular Ca^{2+}, the EC_{50} value in differentiated cells was less than half that in control cells (11.6 and 4.7 μM; control and differentiated cells, respectively). In order to investigate whether this effect may reflect a down-regulation of a Ca^{2+} entry pathway, we used the Mn^{2+} quench technique to directly monitor divalent cation entry induced by the Ca^{2+}-ATPase inhibitor thapsigargin, a classical activator of capacitative Ca^{2+} entry (CCE).

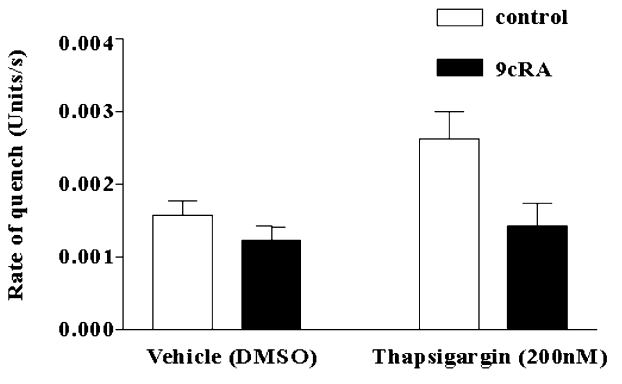

Figure 1. Rate of thapsigargin-induced Mn^{2+} quench in control and 9cRA-differentiated SH-SY5Y cells. Data show fluorescence decrease in units/s; mean ± S.E.M., $n = 6$–8. Unpaired t test, $P < 0.05$.

The results (Fig. 1) showed that both control and differentiated cells exhibit basal levels of Mn^{2+} entry that are not significantly different ($P = 0.24$). However, upon thapsigargin stimulation, control cells showed a significant increase in the rate of Mn^{2+} entry ($P = 0.02$), whereas there was no significant increase following thapsigargin stimulation of differentiated cells ($P = 0.62$). This suggests that whilst in control cells there is a functional CCE pathway that can be stimulated by thapsigargin, in cells differentiated with 9cRA this pathway plays no significant role, and may be shut off or down-regulated.

We are currently investigating whether activation of a CCE pathway such as this could account for the differences in response to methacholine stimulation seen in control cells compared with that seen in 9cRA-differentiated cells.

Bennett, D.L. *et al.* (1998). *Biochem. J.* **329**, 349–357.

Celli, A. *et al.* (1999). *Neurochem. Res.* **24**, 691–698.

Redfern, C.P.F. *et al.* (1995). *Eur. J. Cancer* **31A**, 486–494.

This work is supported by a Programme Grant from the MRC to T.R.C. and a project grant from the NECCRF.

Calcium dependence of human TRPM2 cation channel activation

D. McHugh*, R. Flemming*, S.Z. Xu*, A.M. Scharenberg† and D.J. Beech*

**School of Biomedical Sciences, University of Leeds, Worsley Medical Building, Leeds LS2 9JT, UK and †Department of Pediatrics and Immunology, University of Washington and Children's Hospital and Medical Center, Seattle, Washington, 98195-6320, USA*

TRPM2 is a member of the melastatin-related TRP protein family. It is expressed in the brain, forms a cation channel that is activated by intracellular ADP-ribose and is associated with induction of cell death (Perraud *et al.* 2001; Hara *et al.* 2002). We have further investigated the properties of FLAG-epitope tagged TRPM2 channels stably expressed in HEK-293 cells under the control of a tetracycline inducible CMV promoter. Using Western blotting we found that anti-FLAG antibody detected a single protein band of ~190 kDa only in tetracycline-induced cells. This is the expected size of human TRPM2. Both tetracycline-induced and non-induced cells were studied using calcium imaging and patch-clamp recording. Calcium imaging data are expressed as the change in fura-PE3 ratio ($\Delta R_{340/380}$) for the 340 and 380 nm excitation wavelengths. Patch-clamp recording conditions were similar to those described in Perraud *et al.* (2001). There was 0.05 mM EGTA in the standard patch pipette solution and current amplitudes are given for −100 mV. Functional data are expressed as means ± S.E.M. The n values refer to the number of cells.

Functional expression of TRPM2 was first shown in calcium imaging experiments using protocols similar to those described by Hara *et al.* (2002) but using fura-PE3 as the calcium indicator. A large rise in intracellular calcium occurred in TRPM2-expressing cells after addition of 1 mM hydrogen peroxide to the calcium-containing bath solution ($\Delta R_{340/380} = 0.982 \pm 0.43$; $n = 12$). In non-induced cells there was also a large rise in intracellular calcium, although this was about half the size of that in TRPM2 cells ($\Delta R_{340/380} = 0.438 \pm 0.65$; $n = 15$; $P < 0.05$ when compared with TRPM2 cells using Student's unpaired t test). Because of the size of this background signal we used patch-clamp recording for all other experiments. In non-induced cells with 0.5 mM ADP-ribose in the patch pipette, small currents occurred in the presence of extracellular calcium (−0.073 ± 0.046 nA, $n = 3$). In induced (TRPM2) cells, larger currents occurred with (−9.73 ± 1.361 nA, $n = 5$) than without (0.418 ± 0.227 nA, $n = 5$) ADP-ribose in the pipette. These data

suggest there is tonic as well as ADP-ribose-induced TRPM2 function. We also observed a strong dependence of ADP-ribose-induced TRPM2 currents on calcium. If whole-cell recordings were initiated in the presence of barium, rather than calcium, currents were small (−0.236 ± 0.075 nA, $n = 5$). Moreover, when Ca^{2+} was strongly buffered in the intracellular solution with BAPTA (20 mM) currents were also small (−0.332 ± 0.096 nA, $n = 5$). Cell blebbing associated with TRPM2 currents in the presence of calcium was absent.

From these data we suggest that TRPM2 has some tonic activity in the absence of ADP-ribose and that the ADP-ribose-induced channel activity, which is associated with cell blebbing, is strongly calcium dependent.

Hara, Y. *et al.* (2002). *Mol. Cell.* **9**, 163–173.

Perraud, A.L. *et al.* (2001). *Nature* **411**, 595–599.

We thank the BHF and Wellcome Trust for support

Inhibition of glucose-induced electrical activity in rat pancreatic β-cells by DCPIB, a selective inhibitor of the volume-sensitive anion channel

L. Best, A.P. Yates, K. Sternmeyer† and B. Nilius*

*Department of Medicine, University of Manchester, Manchester M13 9WL, UK, †Aventis Pharma GmbH, Frankfurt am Main, Germany and *Laboratory of Physiology, Catholic University of Leuven, Belgium*

The effects of 4-(2-butyl-6,7-dichloro-2-cyclopentyl-indan-1-on-5-yl) oxobutyric acid (DCPIB), an inhibitor of the volume-sensitive anion channel (VSAC), on the function of pancreatic β-cells were investigated. Rats were killed humanely and islets isolated by collagenase digestion. Islets were then dispersed into single cells by brief exposure to a Ca^{2+}-free buffer. Insulin-secreting β-cells were identified by size and response to glucose. The whole-cell, cell-attached and perforated patch configurations of the patch-clamp technique were used to study ion channel and electrical activity. Insulin release was measured by radioimmunoassay from intact islets.

In 6/6 cells, DCPIB inhibited VSAC activity under conventional whole-cell conditions with IC_{50} values of 2.2 and 1.7 μM for inhibition of outward and inward currents, respectively. DCPIB also suppressed glucose-induced electrical activity in 5/5 β-cells over the concentration range 0.1–10 μM. With lower concentrations of the drug, this inhibitory effect occurred after a longer delay. DCPIB hyperpolarised the cell membrane potential at a sub-stimulatory glucose concentration in 3/3 cells. The suppression of electrical activity by DCPIB was associated with a marked inhibition of glucose-stimulated insulin release from intact islets ($P < 0.01$ at 1 μM DCPIB). K_{ATP} channel activity in cell-attached patches was unaffected by DCPIB, whilst the drug produced a modest, non-significant reduction in whole-cell input conductance, presumably reflecting VSAC inhibition.

It is concluded that DCPIB inhibits electrical and secretory activity in the β-cell as a result of VSAC inhibition and hyperpolarisation of the β-cell membrane potential. This finding strongly supports our earlier suggestion that glucose stimulates β-cell function, at least in part, by activating the VSAC.

All procedures accord with current UK legislation.

Biphasic effects of the fluorescein derivative eosin Y on the human CFTR Cl^- channel

Z. Cai and D.N. Sheppard

Department of Physiology, University of Bristol, Bristol BS8 1TD, UK

The fluorescein derivative phloxine B is a potent modulator of the cystic fibrosis transmembrane conductance regulator (CFTR). Low micromolar concentrations of phloxine B stimulate CFTR Cl^- currents, whereas higher concentrations of the drug inhibit CFTR (Bachmann *et al.* 2000; Cai & Sheppard, 2002). To understand better how fluorescein derivatives modulate the activity of CFTR, we studied eosin Y, an agent with a chemical structure closely related to phloxine B.

We used the patch-clamp technique to investigate CFTR Cl^- channels in excised inside-out membrane patches from C127 cells stably expressing wild-type human CFTR (Cai & Sheppard, 2002). The pipette (external) solution contained 10 mM Cl^-, whereas the bath (internal) solution contained 147 mM Cl^-, PKA (75 nM) and ATP (0.3 mM) at 37 °C; voltage was −50 mV. Following the activation of CFTR Cl^- currents by cAMP-dependent phosphorylation, drugs were added to the intracellular solution. Like phloxine B, low micromolar concentrations of eosin Y (1–5 μM) stimulated CFTR Cl^- currents, whereas higher concentrations of the drug (20–100 μM) inhibited CFTR. For eosin Y, the drug concentration causing half-maximal inhibition of CFTR (K_i) was 48 μM ($n = 4$–16), whereas for phloxine B, K_i was 17 μM ($n = 4$–13). However, the effects of eosin Y were readily reversible, but those of phloxine B only partially reversible.

To learn how eosin Y stimulates and inhibits CFTR, we studied single CFTR Cl^- channels. Eosin Y (1 μM) increased the open probability (P_o; control, $P_o = 0.38 \pm 0.02$; eosin Y, $P_o = 0.43 \pm 0.02$; $n = 8$; means ± S.E.M.; $P < 0.05$; Student's paired t test) without changing either single-channel current amplitude (i) or the number of active channels. Eosin Y (1 μM) increased P_o by prolonging mean burst duration (MBD; control, MBD = 133 ± 7 ms; eosin Y, MBD = 166 ± 11 ms; $n = 4$; $P < 0.05$) without altering the interburst interval (IBI; control, IBI = 194 ± 24 ms; eosin Y, IBI = 201 ± 13 ms; $n = 4$; $P > 0.05$). In contrast, inhibitory concentrations of eosin Y (100 μM) decreased both P_o and i (control, $P_o = 0.38 \pm 0.02$ and $i = -0.78 \pm 0.04$ pA; eosin Y, $P_o = 0.23 \pm 0.02$ and $i = -0.68 \pm 0.04$ pA; $n = 7$; $P < 0.01$ for P_o and i). Eosin Y (100 μM) decreased P_o both by shortening MBD and prolonging IBI (control, MBD = 139 ± 6 ms and IBI = 196 ± 23 ms; eosin Y, MBD = 75 ± 12 ms and IBI = 348 ± 49 ms; $n = 3$; $P < 0.05$ for MBD and IBI). These data indicate that eosin Y is a less potent modulator of CFTR than phloxine B. They also suggest that like phloxine B, eosin Y might interact directly with CFTR at multiple sites to modulate channel activity.

Bachmann, A. *et al.* (2000). *Br. J. Pharmacol.* **131**, 433–400.

Cai, Z. & Sheppard, D.N. (2002). *J. Biol. Chem.* **277**, 19546–19553.

This work was supported by the CF Trust and NKRF.

Investigation of the role of a residue in the S4–S5 linker in the activation of heag potassium channels

M. Ju, L. Rashleigh, M. Aslam and D. Wray

Biomedical Sciences, University of Leeds, Leeds LS2 9JT, UK

Eag channels are members of the *ether-a-go-go* family of potassium channels, and the human eag2 (heag2) channel has been recently cloned and characterised by ourselves (Ju & Wray, 2002) and by Schonherr *et al.* (2002). We compared the steady-state activation properties of this channel with heag1, and found that, in normal potassium solutions, the conductance–voltage (G–V) curve for heag2 is shifted to the left and shows less steep voltage dependence, compared with heag1. Molecular regions that might account for these functional differences may include the S4 transmembrane region or the nearby linkers. However, the S4 region and the S3–S4 linker are identical between the two channels, while there is only one amino acid that is different in the S4–S5 linker: isoleucine in heag1 at position 345 and leucine in heag2. Here we have investigated a possible role of this residue in steady-state activation.

For this, we made the mutation I345L in heag1, using PCR Quickchange mutagenesis. RNA for wild-type heag1 and mutant I345L was injected into *Xenopus* oocytes, and two-electrode voltage-clamp recordings were made at room temperature 2 days later. Cells were held at −80 mV, and depolarising pulses applied at 0.1 Hz (500 ms duration). Current–voltage recordings were made in normal potassium solutions, and Boltzmann curves were fitted to the corresponding G–V curves, parametrised in the usual way (slope parameter k, voltage for half-maximal activation $V_{0.5}$).

For the current–voltage curves, there were no significant differences (Student's unpaired t test) between the currents for wild-type and I345L mutant heag1 channels for a range of test potentials from −30 to +50 mV. Consistent with this, the Boltzmann slope parameter, k, was not significantly different between the two channels (17.1 ± 1.4 mV, $n = 6$, for wild-type; 17.2 ± 1.5 mV for the mutant, $n = 7$, means ± S.E.M.); the $V_{0.5}$ parameter was also not significantly different (9.3 ± 2.1 mV for wild-type, 6.6 ± 1.5 mV for the mutant).

Therefore, the data show that I or L residues (present in heag1 and heag2, respectively) at position 345 in the S4–S5 linker are not involved in the molecular mechanism for the differences between steady-state activation for heag1 and heag2 channels. The result is perhaps not surprising because residues I and L are both amino acids with similar properties such as size, hydrophobicity and neutral charge.

However, residue 345 may be of importance in determining the *kinetics* of activation, which also differs between heag1 and heag2 channels. Further work is in progress therefore to investigate whether this residue in the S4–S5 linker is involved in activation kinetics.

Ju, M. & Wray, D. (2002). *FEBS Lett.* **524**., 204–210.

Schonherr, R. *et al.* (2002). *FEBS Lett.* **514**, 204–208.

All procedures accord with current UK legislation.

The N terminus of ROMK2 is necessary for channel function but not membrane trafficking

V.M. Collins, G.J. Cooper and S.J. White

Department of Biomedical Science, Sheffield University, Western Bank, Sheffield S10 2TN, UK

Alternative splicing of the *KCNJ1* gene in the kidney results in the expression of three major isoforms of the inwardly rectifying K^+ channel ROMK, which differ only in their N-terminal amino acid sequence (Giebisch, 2001). Deletion of amino acids 3–68 of ROMK1 (Kir1.1a) produces non-functional channels that exert a dominant negative effect on wild-type ROMK1 (Koster *et al.* 1998). Here we report the effects of N-terminal deletion of ROMK2 (Kir1.1b) on channel function and membrane trafficking.

Using PCR-based protocols, amino acids 1–56 of rat ROMK2 were deleted. This was subcloned into the *Xenopus* expression vector pTLN (Lorenz *et al.* 1996) and N-terminally tagged with EGFP (EGFP-ROMK2Δ56). Female *Xenopus laevis* were killed humanely and stage V–VI oocytes isolated. Oocytes were injected with 50 nl of RNAse-free H_2O or H_2O containing either 5 ng pTLN-EGFP, EGFP-ROMK2Δ56 or wild-type EGFP-ROMK2 cRNA. Channel activity was assessed 3–4 days after injection at room temperature by measuring currents at a holding potential of 0 mV maintained by two-microelectrode voltage clamp. The bath solution contained (mM): NaCl 96, KCl 2, $MgCl_2$ 1, $CaCl_2$ 1.8, Hepes 5; ± 5 mM $BaCl_2$. The pH of solutions was adjusted to 7.5 ± 0.05 using HCl or NaOH. To determine the cellular location of the EGFP-tagged proteins, the oocytes were fixed in 1% paraformaldehyde and sectioned (10–15 μm thick) using a cryostat at −25 °C. Sections were viewed on a Leica confocal laser-scanning microscope ($\lambda_{Ex} = 488$ nm) within 24 h of sectioning. Data are presented as means ± S.E.M. and statistical significance was determined by one-way ANOVA and Tukey's test.

Oocytes expressing EGFP-ROMK2 displayed Ba^{2+}-sensitive outward currents of 3.06 ± 0.54 μA ($n = 11$). In contrast, oocytes expressing EGFP-ROMK2Δ56 exhibited a Ba^{2+}-insensitive outward current of 0.12 ± 0.01 μA ($n = 10$, $P < 0.05$ cf. EGFP-ROMK2). This current was not significantly different from that of oocytes injected with H_2O (0.13 ± 0.01 μA; $n = 8$) or pTLN-EGFP (0.14 ± 0.01 μA; $n = 8$). Confocal microscopy showed that in oocytes expressing either EGFP-ROMK2 ($n = 4$) or EGFP-ROMK2Δ56 ($n = 4$), the fluorescently tagged proteins were expressed at the plasma membrane. In contrast, fluorescence of oocytes injected either with H_2O or pTLN-EGFP ($n = 3$–5) was solely intracellular.

These results indicate that the N-terminal amino acid sequence (1–56) of ROMK2 is required for normal channel function but is not essential for membrane trafficking of the protein.

Giebisch, G. (2001). *Kidney Int.* **60**, 436–445.

Koster, J.C. *et al.* (1998). *Biophys. J.* **74**, 1821–1829.

Lorenz, C. *et al.* (1996). *PNAS* **93**, 13362–13366.

This work is supported by the National Kidney Research Fund. V.M.C. is a White-Rose Research Student.

All procedures accord with current UK legislation.

The ligand-sensitive gate of a potassium channel lies close to the selectivity filter

Peter Proks, Jennifer F. Antcliff and Frances M. Ashcroft

University Laboratory of Physiology, Parks Road, Oxford OX1 3PT, UK

In ATP-sensitive potassium (K_{ATP}) channels, binding of ATP to the pore-forming Kir6.2 subunit is allosterically linked to closure of the channel pore. To elucidate the location of the gate closed by ATP, we exploited the fact that Ba^{2+} acts as a pore blocker of K^+ channels which binds close to the inner entrance to the selectivity filter (Neyton & Miller, 1988*a, b*; Jiang & MacKinnon, 2000). The rationale is that ATP should slow the rate and reduce the affinity of Ba^{2+} block if the helix-bundle crossing serves as the ATP-sensitive gate, but have no substantial effect if the gate lies above the Ba^{2+}-binding site (e.g. within the selectivity filter). For these experiments, cloned β-cell K_{ATP} channels (Kir6.2/SUR1) were heterologously expressed in *Xenopus laevis* oocytes and currents were recorded from giant inside-out patches at room temperature. The external (pipette) and internal (bath) solutions contained (mM): 107 KCl, 10 EGTA and 10 Hepes; pH 7.2 (with KOH). All data are expressed as means ± S.E.M.

Intracellular Ba^{2+} produced a strong voltage-dependent block of Kir6.2/SUR1 currents, with an IC_{50} of 0.87 ± 0.04 μM ($n = 5$) at +60 mV. Mutation of V129, which is predicted to lie just below the selectivity filter, to threonine (V129T) markedly reduced Ba^{2+} block (IC_{50} = 12.0 ± 0.2 μM; $n = 5$) suggesting Ba^{2+} binds at or near this residue. In both wild-type and V129T mutant channels, ATP dose-dependently accelerated the on-rate and reduced the extent of Ba^{2+} block. This effect is not compatible with the idea that access of Ba^{2+} to its binding site is impaired when the channel is shut by ATP. Simulations of the time course of Ba^{2+} block of macroscopic K_{ATP} currents, based on single-channel data, suggested that Ba^{2+} must be able to access its binding site in both open and closed conformations of the ATP-dependent gate, and that ATP accelerates both on- and off-rate of barium block. This means that the gate closed by ATP lies above the Ba^{2+}-binding site, within or above the selectivity filter. Because Ba^{2+} is almost the same size as K^+, K^+ must also be able to enter the pore when the channel is shut by ATP. Unlike voltage-gated K^+ channels, therefore, the helix-bundle crossing at the inner mouth of the K_{ATP} channel is not a gate for K^+ ions.

Jiang, Y. & MacKinnon, R. (2000). *J. Gen. Physiol.* **115**, 269–272.

Neyton, J. & Miller, C. (1988*a*). *J. Gen. Physiol.* **92**, 549–567.

Neyton, J. & Miller, C. (1988*b*). *J. Gen. Physiol.* **92**, 569–586.

All procedures accord with current UK legislation.

Mapping the architecture of the ATP-binding site of Kir6.2

Michael Dabrowski and Frances M. Ashcroft

University Laboratory of Physiology, Oxford University, Parks Road, Oxford OX1 3PT, UK

ATP-sensitive K^+ (K_{ATP}) channels comprise Kir6.2 and SUR subunits. The site at which ATP binds to mediate K_{ATP} channel inhibition lies on Kir6.2, but the potency of block is enhanced by co-expression with SUR1. To assess the structure of the ATP-binding site on Kir6.2, we used a range of adenine nucleotides as molecular measuring sticks to map the internal dimensions of the binding site. We compared their efficacy on Kir6.2/SUR1, and on a truncated Kir6.2 (Kir6.2ΔC) that expresses in the absence of SUR.

Macroscopic K_{ATP} currents were recorded from giant inside-out membrane patches excised from *Xenopus* oocytes expressing either Kir6.2ΔC or Kir6.2/SUR1, at 18–22°C. The pipette (external) solution contained (mM): 140 KCl, 1.2 $MgCl_2$, 2.6 $CaCl_2$ and 10 Hepes (pH 7.4 with KOH). The intracellular (bath) solution contained (mM): 110 KCl, 2.6 $CaCl_2$, 10 EDTA and 10 Hepes (pH 7.2 with KOH). Nucleotides were added to the intracellular solution. Data are given as means ± 1 S.E.M.

Addition of a ribose moiety to the phosphate tail of ATP or ADP decreased the potency of both nucleotides on Kir6.2ΔC by similar amounts (IC_{50} for ATP from 100 μM to 2.3 ± 0.1 mM, $n = 5$); for ADP from 260 μM to 1.8 ± 0.2 mM, $n = 5$). This suggests that the binding pocket of Kir6.2 is narrower than the ribose moiety at the level of both the second and third phosphates of ATP. Addition of both ribose and adenine moiety to the phosphate tail of ADP (AP2A) largely abolished nucleotide block, suggesting that the binding pocket is not wide enough to accommodate this bulky group at the level of the second phosphate. Remarkably, addition of the ribose/adenine moiety to a three (AP3A), or four (AP4A), phosphate tail partially, or completely, restored nucleotide block: IC_{50} of 538 ± 21 μM, $n = 5$ (AP3A) and 190 ± 18 μM, $n = 6$ (AP4A). This suggests the ATP-binding pocket widens along the length of the phosphate tail, and, in the case of AP4A, the ribose/adenine moiety may lie outside the binding pocket.

SUR1 enhances the potency of ATP ~10-fold (IC_{50} 10 μM). We thus examined if SUR1 modifies the length of the Kir6.2 ATP-binding pocket. Addition of a ribose to the phosphate tail of ATP or ADP decreased the potency of both nucleotides on Kir6.2/SUR1 2- to 3-fold (IC_{50} of 44 ± 5 μM, $n = 5$ (ATP-ribose) and 103 ± 4 μM, $n = 5$ (ADP-ribose)), much less than found for Kir6.2ΔC. There was little difference in the potency of ADP and AP2A on Kir6.2/SUR1 (unlike Kir6.2ΔC). These data suggest that SUR may widen the ATP-binding pocket of Kir6.2 at the level of both the second and third phosphates of ATP, enabling it to accommodate both ribose and adenine moiety. As for Kir6.2ΔC, greater inhibition of Kir6.2/SUR1 was seen with AP3A and AP4A than AP2A, suggesting that the binding pocket is 3–4 phosphates long, and thus does not change when SUR is present.

Endogenous amyloid β protein determines K^+ current expression levels in rat cerebellar granule neurones

L.D. Plant, N.J. Webster*, Z. Henderson, C. Peers* and H.A. Pearson

*School of Biomedical Sciences and *Institute for Cardiovascular Research, University of Leeds, Leeds LS2 9JT, UK*

The A-type potassium current (I_{KA}), mediated by Kv4 subunit containing channels, defines how cerebellar granule neurones (CGN) respond to excitation (An *et al.* 2000). Although tightly regulated, the functional expression of this physiologically important current is enhanced in CGN incubated with exogenous amyloid β protein 1–40 (Aβ; Ramsden *et al.* 2001). Aβ is constitutively derived from amyloid precursor protein by β- and γ-secretase activity and augments I_{KA} via an increase in protein synthesis (Plant *et al.* 2002). Here we use inhibitors of β- and γ-secretase to prevent endogenous Aβ production in CGN and investigate the importance of this peptide to I_{KA}.

Rat cerebellar granule neurones were isolated and cultured from tissue obtained by Schedule 1 methods as previously described (Ramsden *et al.* 2001). For whole-cell patch-clamp recordings,

extracellular and pipette solutions used were those detailed in Ramsden *et al.* (2001). Cells were held at −70 mV and K^+ currents (I_K) evoked by step depolarisations to +50 mV following a prepulse to −140 mV. Western blot analysis of 10 % SDS-PAGE gels was carried out by probing membranes using polyclonal antibodies raised against Kv4.2 and 4.3 α-subunits. All values are given as means ± S.E.M.

In control, untreated granule neurones the mean peak I_K measured at +50 mV was 1.2 ± 0.03 nA pF^{-1} ($n = 17$). This was significantly reduced to 0.58 ± 0.08 nA pF^{-1} ($n = 17$, $P < 0.01$, Student's unpaired t test) following 24 h treatment with 2-Naphthoyl-VF-CHO (γ-IV), an inhibitor of γ-secretase activity. I_K was further diminished (0.36 ± 0.05 nA pF^{-1}, $n = 15$) following 48 h treatment with γ-IV. As γ-secretase activity may contribute to other signalling pathways, the experiment was repeated with H-KTEEISEVN-stat-VAEF-OH (βSI), an inhibitor of β-secretase activity. 24 h treatment with βSI resulted in a decrease in I_K which was similar to that recorded following γ-IV treatment. This suggests that these structurally distinct and secretase selective inhibitors mediate a reduction in I_K via the same pathway. In order to confirm the importance of Aβ to the functional expression of I_K we attempted to rescue the reduction in current caused to γ-IV by co-incubating with 1 nM Aβ. This treatment was effective in negating the deficit in I_K attributed to diminished Aβ production ($I_K = 1.4 \pm 0.05$ nA pF^{-1}, $n = 12$).

These data demonstrate for the first time the importance of endogenous Aβ in determining I_K in central neurones, further supporting the contention that Aβ has a physiological role in the central nervous system.

An, W. *et al.* (2000). *Nature* **403**, 553–556.

Plant, L.D. *et al.* (2002). *Pflügers Arch.* **443**, O17-5.

Ramsden, M. *et al.* (2001). *J. Neurochem.* **79**, 699–712.

This work was supported by the MRC and The Wellcome Trust.

All procedures accord with current UK legislation.

Real-time RT-PCR analysis of K_V1 channel gene expression in mouse aorta

S.J. Fountain, N.D. Quinton, A. Cheong, A. Sivaprasadarao and D.J. Beech

School of Biomedical Sciences, University of Leeds, Leeds LS2 9JT, UK

Voltage-gated potassium channels of the K_V1 subtype provide negative feedback against voltage-dependent calcium entry in vascular smooth muscle (Cheong *et al.* 2001*a, b*). Our aim is to quantify K_V1 mRNA to elucidate mechanisms that regulate expression. Total RNA was isolated from freshly dissected (humanely killed) 8-week-old male mouse aorta after removal of connective tissue and fat, and blood by lumenal perfusion with balanced salt solution. Endothelium was removed by perfusion with Triton-X. Wire myograph recordings demonstrated that the vessels were contractile to 45 mM potassium and phenylephrine. Contractile responses were not diminished after endothelium removal but dilator responses to acetylcholine were abolished. cDNA was synthesized from DNAse I-treated RNA and PCR was performed using gene-specific primers on the Roche Lightcycler combined with SYBR Green detection of dsDNA. Melt-curve analysis and agarose gel electrophoresis were used to determine PCR specificity. Crossing points (C_P) were calculated using Fit Points Method, where C_P corresponds to the PCR cycle at which fluorescence exceeded background signals. Data are given as means ± S.E.M.

Comparison of intact with endothelium-denuded aorta revealed a 10.0 ± 0.1-fold reduction in endothelial nitric oxide synthase (eNOS) mRNA (C_P 27.3 ± 0.1, $n = 3$ cf. 23.9 ± 0.1, $n = 3$; unpaired t test, $P < 0.01$). Levels of β-actin mRNA were similar between intact and denuded aorta (C_P 22.8 ± 0.1, $n = 3$ cf. 22.5 ± 0.0, $n = 3$; $P = 0.04$). $K_V1.1$–1.6, but not KV1.7, mRNAs were detected in endothelium-denuded aorta. Quantitative analysis revealed no change in $K_V1.1$ in denuded compared with endothelium-intact aorta (C_P 31.0 ± 0.2, $n = 3$ cf. 30.9 ± 0.6, $n = 3$; $P > 0.05$). $K_V1.3$ mRNA levels were 5.8 ± 1.0-fold less in denuded compared with endothelium-intact aorta (C_P 32.3 ± 0.7, $n = 3$ cf. 29.5 ± 0.1, $n = 3$; $P < 0.05$). PCR efficiencies were 88 and 94 % for $K_V1.1$ and $K_V1.3$ reactions, respectively. $K_V1.1$–1.6 proteins were detected in smooth muscle of aorta sections by immunostaining with peptide-specific antibodies – $K_V1.1$ and 1.3 signals were the strongest, and $K_V1.4$ and $K_V1.5$ the weakest.

The experiments show the expression of six K_V1 subunits in mouse aorta and demonstrate the potential for using real-time RT-PCR to make quantitative investigations of ion channel mRNA levels in intact and endothelium-denuded arteries. Using this approach we suggest there is $K_V1.1$ mRNA in smooth muscle but not endothelium, whereas $K_V1.3$ mRNA is in both.

Cheong, A. *et al.* (2001*a*). *J. Physiol.* **534**, 691–700.

Cheong, A. *et al.* (2001*b*). *Am. J. Physiol.* **281**, H1057–1065.

We thank the MRC and BHF for support.

All procedures accord with current UK legislation.

Properties of Kv1.3 potassium channels in human lung macrophages

A.B. Mackenzie, H. Chirakkal and R.A. North

Institute of Molecular Physiology, University of Sheffield, Western Bank, Sheffield S10 2TN, UK

The aim of these studies was to identify the voltage-gated potassium channels in human alveolar macrophages and investigate the potential physiological role. Macrophages were obtained from macroscopically normal lung tissue derived from surgical resections, isolated by adherence and identified by morphology. Patients consented to this use of tissue. Whole-cell recordings from cells days 1 to 3 in culture were used to study Kv channel currents. The pipette solution contained (mM): 150 KCl, 10 Hepes and 10 EGTA (pH 7.2) and superfused with saline containing 145 NaCl, 5 KCl, 10 Hepes, 12 glucose, 1 $MgCl_2$ and 2 $CaCl_2$ (pH 7.3). From a holding potential of −100 mV, depolarising pulses activated an outward current, underlying conductance was fitted by a Boltzmann function; $V_{½} = -18 \pm 0.8$ mV and $k = 9.4 \pm 0.75$ mV (means ± S.E.M., $n = 5$). Tail currents reversed around the theoretical value for E_K (extracellular potassium 5 mM, 20 mM and 150 mM) demonstrating a potassium-selective conductance. Margatoxin blocked this outward current with IC_{50} 162 ± 11 pM ($n = 5$), consistent with Kv1.3 (Bednarek *et al.* 1994).

For identification of Kv channel mRNA transcripts, a pure macrophage population was isolated from contaminating myofibroblasts. Macrophages were identified by phagocytosis of BODIPY-labelled, IgG coated zymosan and sorted by flow cytometry. Reverse transcription-polymerase chain reaction (RT-PCR) was performed to detect the transcripts for Kv1.1, Kv1.2, Kv1.3, Kv1.4, Kv1.5, Kv1.6, Kv2.1, Kv2.2, Kv2.3, Kv3.1, Kv3.3, Kv3.4, Kv4.1, Kv4.2 and Kv4.3 channels, only Kv1.3

channel primer pairs gave a product of expected size (269 base pairs).

We sought to determine whether Kv1.3 channels played a role in phagocytosis. In current-clamp recordings, resting membrane potential was -34 ± 1.1 mV ($n = 7$). Exposure to 1 nM margatoxin depolarised the membrane to -4.6 ± 1.1 mV ($n = 5$), suggesting that Kv1.3 channels are involved in setting the resting membrane potential. However, phagocytosis was unaffected; the percentage of cells sorted as macrophages from the total cell population by flow cytometry was 37 ± 7.6 % ($n = 3$) and 35 ± 8.3 % ($n = 3$) for control cells and in the presence of 1 nM margatoxin, respectively. This indicates that functioning Kv1.3 channels are not required for Fc receptor-mediated phagocytosis.

Bednarek, M.A. *et al.* (1994). *Biochem. Biophys. Res. Commun.* **198**, 619–625.

This work was supported by AstraZeneca, Charnwood, UK.

All procedures accord with current local guidelines and the Declaration of Helsinki.

A difference in polyamine permeation of the Kir2.1 and Kir3.1/Kir3.4 inwardly rectifying K^+ channels underlies a difference in inward rectification

T.W. Claydon, S.Y. Makary and M.R. Boyett

School of Biomedical Sciences, University of Leeds, Leeds LS2 9JT, UK

Kir2.1 and Kir3.1/Kir3.4 are inwardly rectifying K^+ channels. We have compared the extent of inward rectification in these channels. Chinese hamster ovary (CHO) cells were transfected with cDNA encoding Green Fluorescent Protein and Kir2.1 or Kir3.1/Kir3.4 and currents were recorded 24–72 h later using the whole-cell patch-clamp technique: 750 ms voltage pulses from −60 to +100 mV were applied from a holding potential of 0 mV at 0.33 Hz. Data were obtained with 140 mM K^+ in both the pipette and bathing solutions. Figure 1 shows normalised current–voltage relationships for Kir2.1 and Kir3.1/Kir3.4. There was less inward rectification in Kir3.1/Kir3.4 than Kir2.1: whereas outward current through Kir2.1 reduced to negligible levels at potentials greater than +60 mV, outward current through Kir3.1/Kir3.4 persisted.

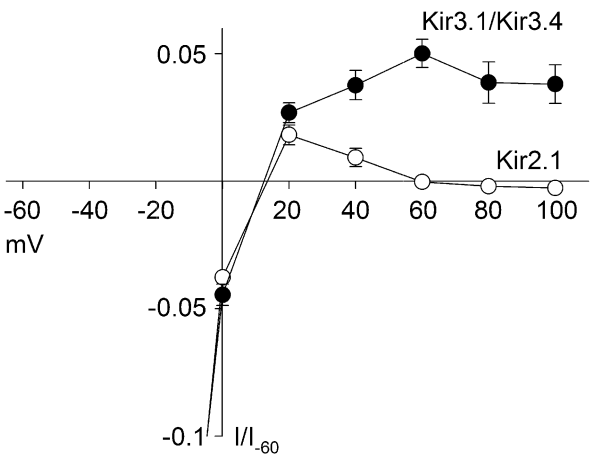

Figure 1. Current–voltage relationships of Kir2.1 and Kir3.1/Kir3.4 channels. Means ± S.E.M. plotted ($n = 5$–7).

Inward rectification involves occlusion of the channel pore by intracellular polyamines, such as spermine. We have investigated the effect of extracellular spermine on Kir2.1 and Kir3.1/Kir3.4 channels expressed in *Xenopus* oocytes. cRNA encoding Kir2.1 or Kir3.1/Kir3.4 was injected into oocytes and currents recorded 16–96 h later using the two-electrode voltage-clamp technique; the voltage-clamp protocol was the same as above, but pulses were applied from −130 to +60 mV. By replacing extracellular K^+ (90 mM) with spermine (90 mM), permeation of the polyamine through each channel was measured. Spermine could not permeate the Kir2.1 channel; sustained current at −130 mV was -0.4 ± 0.6 μA ($n = 10$) with spermine as the main charge carrier (not different from endogenous current; -0.2 ± 0.1 μA, $n = 5$; unpaired t test, n.s.) compared with -14.2 ± 5.2 μA with K^+ as the main charge carrier. In contrast, substantial inward current through the Kir3.1/Kir3.4 channel was measured with spermine as the main charge carrier, suggesting that spermine can permeate the Kir3.1/Kir3.4 channel; current was -2.7 ± 0.6 μA ($n = 6$) with spermine (significantly different from endogenous current; unpaired t test, $P < 0.05$) compared with -11.3 ± 1.3 μA with K^+ as the main charge carrier. These data show that there is less inward rectification in the Kir3.1/Kir3.4 channel than the Kir2.1 channel and we suggest that this is because spermine can permeate the Kir3.1/Kir3.4 but not the Kir2.1 channel.

Interestingly, K^+ current through the Kir3.1/Kir3.4 channel was blocked by extracellular spermine (1–30 mM; 90 mM extracellular K^+ present) more effectively than K^+ current through the Kir2.1 channel; the affinity of spermine for the Kir3.1/Kir3.4 channel was approximately 28-fold greater (at −130 mV; $n = 6$–10) than for the Kir2.1 channel.

This work was supported by the British Heart Foundation.

All procedures accord with current UK legislation.

Chronic hypoxia remodels acute hypoxic inhibition of human maxi-K channels by a differential increase in β-subunit transcription

M.E. Hartness*, C. Peers†, M.L.J. Ashford‡ and P.J. Kemp*

*Schools of *Biomedical Sciences and †Medicine, University of Leeds, Leeds, UK and ‡Department of Pharmacology and Neuroscience, University of Dundee, Dundee, UK*

Prolonged hypoxia regulates the expression of native ion channels (e.g. Colebrooke *et al.* 2002). Whether this functional remodelling also occurs in recombinant systems has yet to be addressed. Here, we report the effects of chronic hypoxia on human recombinant large conductance, Ca^{2+}-activated K^+ (maxi-K) channel activity in human embryonic kidney (HEK 293) cells stably expressing the α and β subunits (Ahring *et al.* 1997).

Cells were cultured as previously described (Lewis *et al.* 2002) in P_{O_2} of either 142 mmHg (normoxia) or 18 mmHg (chronic hypoxia) for 72 h. Whole-cell currents were recorded by the patch-clamp technique using standard 'physiological' solutions and voltage-clamp protocols with $[Ca^{2+}]_i$ buffered to 4 nM, 27 nM, 300 nM or 3 μM. The effect of acute hypoxia was examined by perfusing cells with N_2-bubbled extracellular solution as previously described (Lewis *et al.* 2002).

Consistent with our data from inside-out patches (Lewis *et al.* 2002), inhibition of whole-cell K^+ currents by acute hypoxia was $Ca^{2+}{}_i$-dependent; at low levels (4 nM) of $Ca^{2+}{}_i$, K^+ current displayed no significant acute hypoxic inhibition whilst at higher levels (> 27 nM), acute hypoxia always depressed K^+ currents.

Chronic hypoxia increased K^+ current density at all $[Ca^{2+}]_i$. For example, at 27 nM, chronic hypoxia caused an increase from 56.0 ± 7.1 pA pF^{-1} (mean ± S.E.M., $n = 10$) to 108.3 ± 14.9 pA pF^{-1} (measured at +60 mV; $P < 0.005$, Student's unpaired t test). Importantly, chronic hypoxia dramatically modulated the Ca^{2+} sensitivity of the acute hypoxic response such that hypoxic inhibition of K^+ current could now be seen at low $[Ca^{2+}]_i$. For example, at 4 nM, acute hypoxic inhibition was 1.1 ± 3.4 % ($n = 8$) in normoxic cells and a 15.5 ± 5.0 % ($n = 8$, $P < 0.05$) in chronic hypoxic cells; this functional remodelling was prevented by pretreatment with 5 mg ml^{-1} actinomycin D ($n = 5$). Western blotting showed that α subunit expression was unaffected by chronic hypoxia, whilst β subunit expression was increased by 324.0 ± 42 % ($n = 6$, $P < 0.05$); as with the functional assay, this augmentation was prevented by actinomycin D ($n = 4$). Finally, immunocytochemistry, employing confocal microscopy, showed that chronic hypoxia increased plasma membrane colocalisation of the α and β subunits and strengthens the argument that modulation of the acute hypoxic response of maxi-K channels by chronic hypoxia is due to differential transcriptional upregulation of the β subunit.

Ahring, P.K. *et al.* (1997). *FEBS Lett.* **415**, 67–70.

Colebrooke, R.L. *et al.* (2002). *Neurosci. Lett.* **318**, 69–72.

Lewis, A. *et al.* (2002). *J. Physiol.* **540**, 771–780.

This work was funded by British Heart Foundation and The Wellcome Trust.

Identification and expression of intermediate- and small-conductance calcium-activated potassium channels in rat small mesenteric arteries: relevance to endothelium-derived hyperpolarising factor (EDHF)

J.M. Hinton and P.D. Langton

Department of Physiology, University of Bristol, School of Medical Sciences, Bristol BS8 1TD, UK

Combinations of the K^+ channel inhibitors apamin and charybdotoxin (CHTx) (Waldron & Garland, 1994) and apamin and maurotoxin (MTx) (Hinton & Langton, 2001) abolish EDHF-mediated relaxation of rat isolated mesenteric arteries. The site of action of these toxins is on the endothelium (Doughty *et al.* 1998), suggesting that membrane hyperpolarisation is via opening of endothelial K^+ channels in these arteries. Apamin inhibits small-conductance calcium-activated K^+ (SK) channels, while CHTx and MTx inhibit intermediate-conductance calcium-activated K^+ (IK) channels and some voltage-gated K^+ channels. In the present study, we examined the identification and expression of IK and SK channels in rat small mesenteric arteries.

Male Wistar rats (200–250 g) were stunned and killed by cervical dislocation, mesenteric arteries of third and forth order branches were dissected free and cleaned of connective tissue. In isometrically mounted arteries contracted with phenylephrine (0.5–2 μM), acetylcholine (ACh, 0.01–10 μM) elicited concentration-dependent relaxation in the presence of *N*-nitro-L-arginine methyl ester (100 μM) and indomethacin (2.8 μM), inhibitors of NO synthase and cyclo-oxygenase, respectively. This relaxation was abolished by combinations of CHTx plus apamin, and MTx plus apamin (each, 50 nM; $n = 6$), application of the toxins alone had no effect. The scorpion toxin SK inhibitors, PO5 toxin and TS Kappa toxin (each, 50 nM; $n = 6$) alone had no significant effects, and in combination with either CHTx or MTX (each 50 nM, $n = 6$) there was no further effect on EDHF-mediated relaxation.

Western blotting of arterial homogenates using anti-SK2 and SK3 (Alomone Laboratories) demonstrated several bands, none at the predicted molecular weight for SK2 or SK3. Subsequent immunoconfocal microscopy of arterial sections using these antibodies demonstrated diffuse and inconclusive antibody staining throughout the arterial wall.

These data demonstrate the involvement of IK channels in EDHF-mediated relaxation of rat isolated mesenteric arteries. However, the identity and role of endothelial SK channels in these arteries remains unclear.

Doughty, J.M. *et al.* (1998). *Am. J. Physiol.* **276**, 1107–1112.

Hinton, J.M. & Langton, P.D. (2001). *J. Physiol.* **536.P**, 112*P*.

Waldron, G.J. & Garland, C.J. (1994). *Can. J. Physiol. Pharmacol.* **72** suppl. 1, 11.

We thank the BHF for financial support (PG/99/70).

All procedures accord with current UK legislation.

Membrane targeting and voltage gating of connexin 26 and 30 fused to GFP colour variants

M. Beltramello*†‡, V. Piazza*†‡ and F. Mammano*†

**Venetian Institute of Molecular Medicine (VIMM), University of Padova, Padova, Italy, †INFM Unit, Research Line TSB2, Trieste, Italy and ‡IRRCS Casa Sollievo della Sofferenza, San Giovanni Rotondo, Foggia, Italy*

The connexin (Cx) family of proteins form gap junctional channels that allow intercellular transfer of small molecules and ion currents. Some genes of the Cx family, particularly Cx26 (*GJB2*), Cx31 (*GJB3*) and Cx30 (*GJB6*) have been implicated in hereditary deafness. Although most of these mutations are associated with a complete loss of function, some of them do retain the ability to form functional channels (Ressot *et al.* 1998). Cx26 and Cx30 are abundantly expressed amongst supporting cells of the organ of Corti in the cochlea (Lagostena *et al.* 2001).

In an effort to unravel the molecular mechanisms underlying the development of a pathological phenotype in the presence of mutated function channels, we molecularly engineered fluorescent chimeric constructs formed by Cx26 and Cx30 each genetically fused to the cyan (ECFP) and yellow (Venus) colour variants of the green fluorescent protein (GFP). The cDNA of Cx26 and 30 was amplified from genomic DNA deleting the authentic Cx stop codons. The 3′ end of Cx cDNAs was then fused to the 5′ end of the GFP mutant cDNA through a linker coding for six amino acids (DPPVAT) and cloned in pcDNA3.1zeo+ transfection vectors (Invitrogen, Carlsbad, CA, USA). Transient transfection was performed on cultures of communication-deficient human cervical carcinoma (HeLa) cells grown to 50–75 % confluency in Opti-MEM medium (Invitrogen) containing lipofectamin (Invitrogen) and 1 μg of plasmid DNA. Living cells co-transfected with Cx26-Venus and Cx30-ECFP constructs were illuminated by the 457 nm (ECFP) and 514 nm (Venus) lines of the Argon laser in a BioRad 2100 confocal microscope with emission filter settings that minimized the bleed-through of the cyan and yellow channels. Image analysis revealed extensive co-localization of the two Cx types in

the same gap junction plaques formed by constructs which appeared correctly targeted at the plasma membrane of contact regions between adjacent cells (Fig. 1*A*).

HeLa cells transfected with the Cx26-Venus and Cx30-Venus constructs were additionally used to obtain dual patch clamp recordings. Cell pairs visually identified as connected by fluorescent plaques revealed that these gap junctions contained functional channels, which also exhibited the correct dependence of junctional conductance on transjunctional voltage (Fig. 1*B*) and were blocked by application of CO_2 (100 %) or carbenoxolone (75 μM; Fig. 1*C*). Voltage gating properties were investigated by subjecting one of the two cells to ramps of potential from the holding potential (0 mV) to ±120 mV and recording the whole-cell current in the unstimulated cell. Peak conductances (measured around 0 mV) were 0.55 ± 0.15 nS and 3.8 ± 1.2 nS in Cx26 ($n = 3$ pairs) and Cx30 ($n = 4$ pairs) transfectants, respectively. When measured with ramp speeds in the range 100–200 ms mV^{-1}, conductance half-inactivation voltages were (in absolute value) 55 ± 3 mV (Cx26) and 38 ± 2 mV (Cx30). These preliminary results indicate that the combination of molecular biology, fluorescence microscopy and electrophysiology may pave the way to the identification of Cx functional deficits relevant to hearing impairment.

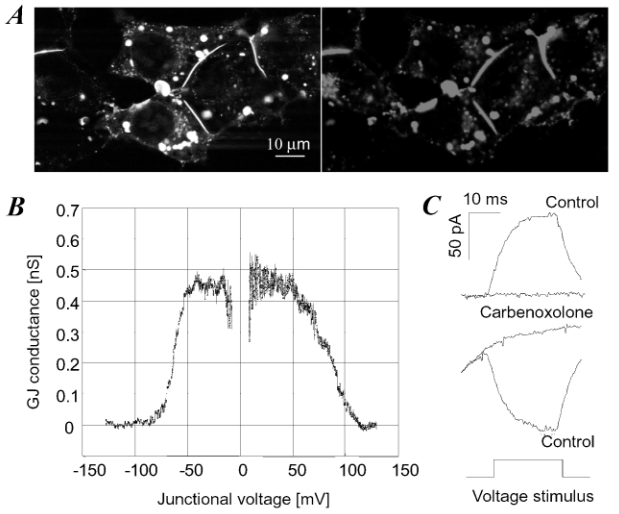

Figure 1. Expression of fluorescent functional Cx chimeras in HeLa cells. *A*, Cx26-Venus (left) and Cx30-ECFP (right) constructs visualized in the same field using the 457 nm and 514 nm Ar lines, respectively. *B*, gap junction conductance of the Cx26-Venus chimeras plotted *vs.* transjunctional voltage; recordings were obtained using 100 ms mV^{-1} voltage ramps from −120 to +120 mV. *C*, Cx26-Venus junctional currents evoked by 100 mV steps in control conditions and during bath application of the gap junction blocker carbenoxolone (75 μM).

Lagostena, L. *et al.* (2001). *Cell Comm. Adhesion* **8**, 17.

Ressot, C. *et al.* (1998). *J. Neurosci.* **18**, 4063–4065.

This work was supported by grants from the INFM (R.L. TSB2) and MIUR to F.M. and Tullio Pozzan. M.B. and V.P. were supported by fellowships from the IRCSS S.G.R.

$GABA_A$ receptor activation increases $[Ca^{2+}]_i$ via a nifedipine-sensitive pathway in cultured rat cerebellar granule neurones

Robert B. Liversage, Leigh D. Plant, Hugh A. Pearson, David J. Beech and Alan N. Bateson

School of Biomedical Sciences, University of Leeds, Leeds LS2 9JT, UK

$GABA_A$ receptor activation can have an excitatory action in developing neurones, associated with a reversal of the Cl^- electrochemical gradient (Owens *et al.* 1996). During this early developmental period, depolarising GABAergic potentials increase $[Ca^{2+}]_i$, a key regulator of gene expression (Ghosh & Greenberg, 1995). It has been previously shown that $GABA_A$ receptor gene expression is altered upon long-term receptor activation, although the cellular mechanisms remain unknown (Holt *et al.* 1997). Here we provide data on $GABA_A$ receptor-mediated $[Ca^{2+}]_i$ changes in 3 day *in vitro* cultured rat cerebellar granule neurones (CGN). Rats were killed by cervical dislocation according to Schedule 1 procedures.

Neuronal $[Ca^{2+}]_i$ of CGN, isolated from 6- to 8-day-old pups, was measured using fluorescence from the calcium indicators fura-PE3 or fluo-4. Normal and drug-supplemented bath solutions were delivered at room temperature with a rapid exchange bath perfusion system (4 ml min^{-1}). Data are given as means ± S.E.M. (using n values), where n represents the number of neurone recordings and y represents the number of individual experiments.

Administration of the selective $GABA_A$ receptor agonist muscimol (0.1 mM, $n = 54$, $y = 3$) or the non-selective GABA receptor agonist GABA (0.1 mM, $n = 54$, $y = 3$) both caused a rapid, transient increase in $[Ca^{2+}]_i$. The EC_{50} for GABA was 0.06 mM ($n = 201$, $y = 20$). The $GABA_B$ receptor agonist baclofen (0.1 mM) produced little or no effect ($n = 58$, $y = 3$), demonstrating that $GABA_B$ receptors are not involved. The selective $GABA_A$ receptor antagonists (0.01 mM) picrotoxin and gabazine blocked the 0.1 mM muscimol-induced $[Ca^{2+}]_i$ response by 30.2 ± 12 % ($n = 53$, $y = 3$) and 76.4 ± 10 % ($n = 59$, $y = 3$), respectively.

The L-type Ca^{2+} channel blocker nifedipine (0.01 mM) attenuated the muscimol-induced $[Ca^{2+}]_i$ response by 91 ± 4 % ($n = 45$, $y = 3$), with the peak $[Ca^{2+}]_i$ rise occurring 70 ± 10 s later than the peak muscimol-induced $[Ca^{2+}]_i$ response.

From these data we conclude that the $[Ca^{2+}]_i$ of CGN increases upon activation of $GABA_A$, rather than $GABA_B$ receptors. This occurs via a nifedipine sensitive pathway, suggesting that $GABA_A$ receptor activation might cause depolarisation which in turn activates L-type voltage-sensitive Ca^{2+} channels. These data along with the established role of Ca^{2+} in regulating gene expression suggest a possible pathway for $GABA_A$ receptor activation to modify its own gene expression in immature neurones.

Ghosh, A. & Greenberg, M.E. (1995). *Science* **268**, 239–247.

Holt, R.A. *et al.* (1997). *Mol. Brain Res.* **48**, 164–166.

Owens, D.F. *et al.* (1996). *J. Neurosci.* **16**, 6414–6423.

R.B. Liversage has a MRC PhD Sudentship.

All procedures accord with current UK legislation.

Homology modelling and molecular dynamics simulations of a prokaryotic glutamate receptor: GluR0

Yalini Arinaminpathy and Mark S.P. Sansom

Laboratory of Molecular Biophysics, Department of Biochemistry, South Parks Road, University of Oxford, Oxford OX1 3QU, UK

Ionotropic glutamate receptors (iGluRs) mediate excitatory synaptic events in the central nervous system of vertebrates. iGluRs and K^+ channels are thought to share a common transmembrane (TM) topology in their core pore-forming domains (Wood *et al.* 1995). A prokaryotic K^+-selective glutamate receptor (GluR0) has significant homology with the bacterial K^+ channel KcsA (Chen *et al.* 1999). Therefore, the structure of the pore-forming domain of KcsA may be used as a template for homology modelling the equivalent domain in GluR0. A homology model of the transmembrane region of GluR0 was generated using Modeller6 based on the X-ray structure (2.0 Å) of KcsA (Zhou *et al.* 2001). Two initial models were generated, based on slightly different (in the loop/P-helix region) sequence alignments. On the basis of initial molecular dynamics (MD) simulations, the model that gave the lowest structural drift was selected for further analysis. This model was used as the starting point for further analysis and for MD simulations. The distribution of charged residues in GluR0 (see Fig. 1) compared with that in KcsA indicates a similarity between the models.

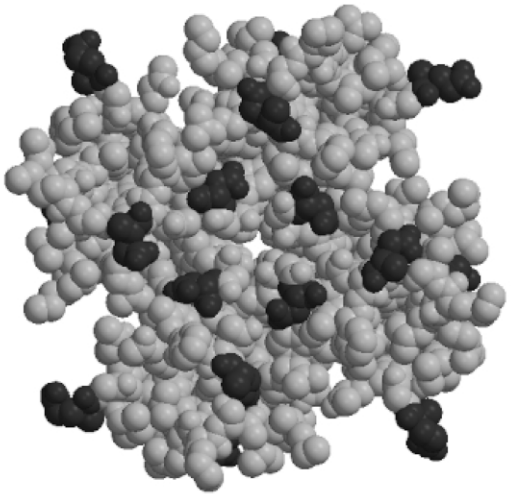

Figure 1. Molecular surface of GluR0. Acidic residues are highlighted in dark grey. The view is down the pore axis from the intracellular mouth of the protein.

Figure 2. Schematic diagram of GluR0, viewed perpendicular to the pore axis with the intracellular end at the top. Amphipathic aromatic residues (Trp and Tyr) are shown in dark grey.

The GluR0 model was inserted into a pre-equilibrated octane slab (a mimic of a lipid bilayer) and the system was solvated and counter-ions added to ensure overall electroneutrality. The positioning of K^+ in the crystal structure of KcsA was replicated in our model. The protein and ions were then subjected to a protein-restrained MD run of 400 ps after which an unrestrained production simulation was run for 6 ns. Structural drift of the GluR0 model from its initial conformation and structural fluctuations assessed over the course of the simulation revealed no significant fluctuations in the filter and the TM helices, in particular the M2 and P helix. This is consistent with hydrogen-bond analysis, which revealed long-lived interactions involving residues in close-proximity to the filter region and the existence of four inter-subunit salt bridges (Asp213-Arg217) also near the filter region. Similar interactions are observed in KcsA (Asp80–Arg89) and are thought to maintain the relative rigidity of the filter, which is an essential component for K^+ selectivity. The concerted single-file motion of K^+ within the filter of GluR0 was similar to that observed in KcsA simulations (Sansom *et al.* 2000). Analysis of the filter region revealed minor structural fluctuations during the concerted motion of ions, which also correlates well with the behaviour of the filter in KcsA. This homology modelling and simulation study of GluR0 provides an insight into the dynamic behaviour of K^+-selective GluR0. A number of similarities between KcsA and GluR0 were revealed. In particular, this study has indicated that the M1, P and M2 pore-forming regions in GluR0 and KcsA have similar architectures and possibly similar functional roles.

Chen, G.-Q. *et al.* (1999). *Nature* **402**, 817–821.

Sansom, M.S.P. *et al.* (2000). *TIBS* **25**, 368–384.

Wood, M.W. *et al.* (1995). *Proc. Natl Acad. Sci. USA* **92**, 4882–4886.

Zhou, Y. *et al.* (2001). *Nature* **414**, 43–48.

This work was supported by the MRC, Wellcome Trust and OSC.

Co-localization of voltage-gated sodium channel α- and β-subunits in adult mouse ventricular myocytes

Sebastian Maier, Ruth Westenbroek, Todd Scheuer and William A. Catterall

Department of Pharmacology, University of Washington, Box 357280, Seattle, WA 98195, USA

Voltage-gated sodium channels isolated from mammalian tissue are composed of the pore-forming α- and auxiliary β-subunits. However, the composition of sodium channels in cardiac muscle has not been defined completely and uncertainty exists as to which α- and β-subunits co-localize at the cellular level in cardiac myocytes.

Using immunocytochemistry and confocal microscopy in isolated adult mouse cardiomyocytes (from humanely killed animals), we investigated the isoform-specific localization of sodium channel α- and auxiliary β-subunits in relation to marker proteins. Anti-Connexin 43 and anti-α-actinin antibodies were used to identify the region of the intercalated disks and the t-tubules, respectively. We find that, in addition to the cardiac α-isoform (Nav1.5), three major brain isoforms, Nav1.1, Nav1.3 and Nav1.6, are also present in ventricular myocytes ($n > 10$). These isoforms are localized differently within single cardiomyocytes: Nav1.5 is found at the intercalated discs, whereas staining for Nav1.1, Nav1.3 and Nav1.6 is striated, suggesting that it is within the transverse tubules at the z-lines. These locations were confirmed as α-actinin was colocalized with the expressed brain-type sodium channels, whereas connexin 43 staining pattern overlapped that of Nav1.5. The brain isoform, Nav1.2, could not be detected in our preparation ($n > 10$). All known auxiliary β-subunits (β1, β2, β3) were also found in adult mouse ventricular myocytes ($n > 10$), and these too displayed differential localisation on the myocytes. β1 and β3 colocalize in the t-tubules with α-actinin, whereas β2 is present at the intercalated disks, colocalized with connexin 43 ($n > 10$).

In summary, we show that the brain-type α-subunits colocalize with β1 and β3 in the transverse tubular system, and Nav1.5 with β2 in the intercalated disks. Our results suggest that the primary sodium channel complexes present in ventricular myocytes consist of Nav1.5 α associated with β2 subunits in the intercalated disks and Nav1.1, Nav1.3 and Nav1.6 associated with β1 or β3 subunits in the t-tubules.

All procedures accord with current National and local guidelines.

Mechanism of niflumic acid inhibition of the human CFTR Cl^- channel

T.S. Scott-Ward, H. Li, A. Schmidt† and D.N. Sheppard

Department of Physiology, University of Bristol, Bristol, UK and †Centre of Human Genetics, National Institute of Health Dr Ricardo Jorge, Lisboa, Portugal

The arylaminobenzoate niflumic acid (NFA) is widely used to inhibit Ca^{2+}-activated Cl^- channels (White & Aylwin, 1990). NFA shares a high degree of structural homology with another arylaminobenzoate, diphenylamine-2-carboxylate (DPC), which inhibits a variety of Cl^- channels including the cystic fibrosis transmembrane conductance regulator (CFTR; McCarty *et al.* 1993).

We investigated the effect of NFA on the CFTR Cl^- channel using inside-out membrane patches excised from C127 cells stably expressing wild-type human CFTR (Lansdell *et al.* 2000). The pipette (external) solution contained 10 mM Cl^- and the bath (internal) solution contained 147 mM Cl^-, 0.3–5 mM ATP and 75 nM PKA at 37°C; voltage was −50 mV. We expressed data as means ± S.E.M. of n observations and performed statistical analyses using Student's paired t tests. Addition of NFA to the intracellular solution caused a concentration-dependent decrease of CFTR Cl^- current with half-maximal inhibitory concentration (K_i) of 253 ± 16 μM and Hill coefficient of 0.95 ± 0.03 ($n = 5$); inhibition was readily reversible.

At the single-channel level, NFA (200 μM) caused a very fast, flickery block of CFTR that dramatically decreased current amplitude (i; control, −0.80 ± 0.03 pA; NFA (200 μM), −0.36 ± 0.04 pA; $n = 5$; $P < 0.01$), but was without effect on open probability ($n = 5$; $P > 0.35$). To investigate how NFA inhibits CFTR, we performed experiments to distinguish between allosteric and open-channel block. CFTR inhibition by the allosteric blocker genistein is relieved by elevated concentrations of ATP (Lansdell *et al.* 2000). In the presence of ATP (0.3 and 5 mM), NFA (200 μM) decreased CFTR Cl^- current to 43 ± 2 and 49 ± 2% of the control value ($n = 6$), respectively. These data suggest that NFA does not inhibit CFTR by an allosteric mechanism. To learn whether NFA is an open-channel blocker of CFTR, we examined the voltage dependence of NFA inhibition of CFTR. When the external [Cl^-] was 10 mM, the voltage-dependent dissociation constant (K_d) for NFA inhibition of CFTR decreased from 391 ± 60 μM at 0 mV to 179 ± 23 μM at −100 mV ($P < 0.05$, $n = 5$) and the electrical distance sensed by NFA (δ) was 0.20 ± 0.03 ($n = 5$) when measured from the intracellular side of the membrane over the voltage range −100 to −40 mV. These data indicate that NFA inhibition of CFTR is voltage dependent and that the drug binding site is located within the electric field of the membrane. These data suggest that NFA is an open channel blocker of CFTR.

Lansdell, K.A. *et al.* (2000). *J. Physiol.* **524**, 317–330.

McCarty, N.A. *et al.* (1993). *J. Gen. Physiol.* **102**, 1–23.

White, M.M. & Alywin, M. (1990). *Mol. Pharmacol.* **37**, 720–724.

This work was supported by the CF Trust and NKRF.

Multiple effects of intracellular pH on the activity of the human CFTR Cl^- channel

J.H. Chen, Z. Cai and D.N. Sheppard

Department of Physiology, University of Bristol, Bristol BS8 1TD, UK

The cystic fibrosis transmembrane conductance regulator (CFTR) is a Cl^- channel with complex regulation. Channel gating is controlled by two nucleotide-binding domains and an R (regulatory) domain located on the cytoplasmic side of the cell membrane. The location of these domains suggests that their function might be regulated by intracellular pH. To test this hypothesis, we investigated the effect of changing intracellular pH on the activity of CFTR.

In this study, we used the patch-clamp technique to investigate CFTR Cl^- channels in excised inside-out membrane patches from C127 cells stably expressing wild-type human CFTR (Lansdell *et al.* 2000). The pipette (external) solution contained 10 mM Cl^- at pH 7.3, whereas the bath (internal) solution contained 147 mM Cl^-. To ensure that the Cl^- concentration was identical, all bath solutions were first titrated to pH 7.3 (control) with HCl before adding either H_2SO_4 to decrease pH or Tris to increase pH. Voltage was clamped at −50 mV and the bath solution was maintained at 37°C. To stimulate and sustain the

activity of CFTR Cl^- channels, PKA (75 nM) and ATP (0.3–1 mM) were added to all internal solutions. We expressed data as means ± S.E.M. of *n* observations and performed statistical analyses using Student's paired *t* test.

We began by investigating the effects of changing intracellular pH on CFTR Cl^- currents. When the internal solution was acidified, the magnitude of CFTR Cl^- current increased (pH 7.3, 100 %; pH 6.3, 141 ± 9 %; $n = 6$; $P < 0.001$). In contrast, when the internal solution was alkalinised, the magnitude of CFTR Cl^- current decreased (pH 7.3, 100 %; pH 8.3, 70 ± 9 %; $n = 6$; $P < 0.001$). The effects of acid and alkaline pH on CFTR Cl^- currents were reversible. To investigate how intracellular pH regulates CFTR, we studied single CFTR Cl^- channels. At pH 6.3, the duration of channel openings was increased and the length of the long closures separating channel openings was decreased. As a result, at pH 6.3 the open probability (P_o) of CFTR was greatly increased (pH 7.3, $P_o = 0.44 \pm 0.02$; pH 6.3, $P_o = 0.62 \pm 0.02$; $n = 5$; $P < 0.001$). In contrast, at pH 8.3 the duration of channel openings decreased and the length of the long closures separating channel openings was increased. As a result, at pH 8.3, the P_o of CFTR was markedly decreased (pH 7.3, $P_o = 0.42 \pm 0.02$; pH 8.3, $P_o = 0.29 \pm 0.03$; $n = 8$; $P < 0.001$). Moreover, at pH 8.3 the single-channel current amplitude of CFTR was decreased (pH 7.3, −0.85 ± 0.02 pA; pH 8.3, −0.81 ± 0.02 pA; $n = 8$; $P < 0.001$). Acidifying the intracellular solution was without effect on *i* ($n = 5$). These data indicate that intracellular pH has multiple effects on the single-channel activity of CFTR. They also suggest that several protein regions within CFTR might contain pH-sensitive amino acid residues.

Lansdell, K.A. *et al.* (2000). *J. Physiol.* **524**, 317–330.

This work was supported by the CF Trust and the University of Bristol.

F-channel-dependent modulation of cardiac SAN activity in the presence and absence of ryanodine

Annalisa Bucchi*, Mirko Baruscotti*, Richard B. Robinson† and Dario DiFrancesco*

**Università di Milano, Dipartimento di Fisiologia e Biochimica Generali, via Celoria 26, 20133 Milano, Italy and †Columbia University, Department of Pharmacology, New York, USA*

Mammalian cardiac impulse is generated in sinoatrial node (SAN) cells, and its automaticity is sustained by a complex interplay of different ionic currents. Evidence in cardiac and neuronal tissues points to the 'funny' (I_f) current as a major player both in pacemaker generation and its modulation by autonomic transmitters (DiFrancesco, 1993). However, the relative importance of individual ionic components in pacemaking is still debated. Recent data indicate a role for Ca^{2+} release from the sarcoplasmic reticulum (SR) in pacemaker activity (Terrar & Rigg, 2000). Based on evidence that disruption of ryanodine receptor (RyR) function abolishes Ca^{2+} transients and β-receptor (β-R)-induced modulation of heart rate, Vinogradova *et al.* (2002) proposed a novel Ca^{2+}-dependent, I_f-independent mechanism of pacemaker regulation by β receptors relying on the activation of subsarcolemmal RyRs.

To check if the I_f-dependent rate-regulation mechanism is still operating after impairment of RyR function, we measured the spontaneous rate from single rabbit SAN cells (or small groups of cells) before and during perfusion with ryanodine (3 μM). In agreement with previous data, the spontaneous rate was decreased by ryanodine (31.0 ± 3.3 %, $n = 5$; mean ± S.E.M.). In the presence of ryanodine (2–3 min exposure), the action of isoprenaline (ISO, 1 μM) on rate was strongly reduced, although not fully abolished (11.4 ± 2.0 *vs.* 26.4 ± 2.0 % in control, $n = 4$). To test if the reduction of ISO effect involved a decreased cAMP availability, we used a membrane-permeable cAMP analogue (pCPT-cAMP, 100 μM) and found that the mean frequency increase induced by pCPT-cAMP in ryanodine-treated cells (20.0 ± 3.6 %) did not change significantly with respect to control (22.5 ± 6.8 %) ($n = 3$). This suggests that the I_f-dependent rate-modulation pathway is still operating in ryanodine-treated cells. However, as well as activating I_f channels directly (DiFrancesco, 1986), pCPT-cAMP could also activate phosphorylation-dependent mechanisms by activation of protein kinase A (PKA). In an attempt to discriminate between phosphorylation-dependent and phosphorylation-independent processes, preliminary experiments using Rp-cAMPs, a cAMP analogue unable to activate PKA and known to activate I_f channels (Bois *et al.* 1997), suggest that ryanodine does not reduce the rate increase caused by Rp-cAMPs: 50 μM Rp-cAMPs increased the rate by 18 % in control conditions, and by 22 % after ryanodine treatment in two cells.

Our data support the view that ryanodine treatment does not impair the cAMP-dependent mechanism of rate modulation mediated by I_f channels. Disruption of RyR function and depletion of Ca^{2+} stores by ryanodine may impair the β-R modulation of rate by reducing the ability of β-R stimulation to induce cAMP synthesis.

Bois, P. *et al.* (1997). *J. Physiol.* **501**, 565–571.

DiFrancesco, D. (1986). *Nature* **324**, 470–473.

DiFrancesco, D. (1993). *Annu. Rev. Physiol.* **55**, 451–476.

Terrar, D. & Rigg, L. (2000). *J. Physiol.* **524**, 316.

Vinogradova, T.M. *et al.* (2002). *Circ. Res.* **90**, 73–79.

This work was supported by Cofin 2000 to D.D. R.B.R. was supported by NIH grant HL-28958.

All procedures accord with current National guidelines.

Blockers of store-operated channels (SOCs) in pial arteriolar smooth muscle cells of rabbit

R. Flemming and D.J. Beech

School of Biomedical Sciences, University of Leeds, Leeds LS2 9JT, UK

SOCs are a distinct class of Ca^{2+}-permeable channel in smooth muscle cells of cerebral arterioles (Flemming *et al.* 2002). TRPC1 is involved in the function of these SOCs but other molecular elements are unknown (Xu & Beech, 2001). In this study we explored the sensitivity of the SOCs to a range of blockers.

Male rabbits were killed by an I.V. overdose of sodium pentobarbitone according to Schedule 1 procedures. Arteriolar fragments were isolated from pial membrane and loaded with fura-PE3. $[Ca^{2+}]_i$ was measured by ratiometric imaging from smooth muscle cells in arterioles. Effects of LOE908 were studied using fluo-4. Except when the effects of 60 mM K^+ were studied, solutions contained 0.01 mM methoxyverapamil to block voltage-gated Ca^{2+} channels. Store depletion was induced using 1000 nM thapsigargin or 0.01 mM cyclopiazonic acid. Data are expressed as means ± S.E.M. The *n* values refer to the number of cells. The number of individual arterioles was at least three for each data set.

Store depletion induced sustained Ca^{2+} entry that depended on extracellular Ca^{2+}. It was strongly inhibited by bath-applied 0.01 mM Gd^{3+} (97.2 ± 2.1 %, $n = 24$ cells), 0.01 mM La^{3+}

(70.4 ± 8.7 %, $n = 21$) or 0.1 mM Ni^{2+} (56.8 ± 10.9 %, $n = 19$). Gd^{3+} and Ni^{2+} had no effect on $[Ca^{2+}]_i$ in the absence of store depletion ($n = 43$ and 23) and, although La^{3+} had an effect, the absolute size of this effect was small (24 % of that in store-depleted cells, $n = 15$). 2-Aminoethoxydiphenylborate (0.075 mM) inhibited SOC-mediated Ca^{2+} entry in 67 % of cells (66.5 ± 2.7 % inhibition, $n = 20$) with no effect in controls ($n = 35$). A 1 h pre-incubation with wortmannin (0.01 mM) strongly inhibited the Ca^{2+} re-entry signal in store-depleted cells ($\Delta R_{340/380}$ 0.017 ± 0.004, $n = 20$ *vs.* 0.093 ± 0.017, $n = 18$; $P < 0.05$, Student's unpaired *t* test).

SOCs in smooth muscle cells of choroidal arterioles are blocked by nifedipine (Curtis & Scholfield, 2001). Nifedipine (1000 nM) abolished the $[Ca^{2+}]_i$ rise in response to 60 mM K^+ (91.5 ± 4.1 %, $n = 19$) but had no effect on SOC-mediated Ca^{2+} entry ($n = 24$). SOC-mediated Ca^{2+} entry was slightly inhibited (< 15 %) or resistant to other inhibitors: 0.01 mM SKF96365 ($n = 16$); 0.01 mM LOE908 ($n = 56$); 0.1 mM ruthenium red ($n = 10$); 0.1 mM capsaicin ($n = 10$); 0.1 mM sulindac ($n = 19$); 0.5 mM streptomycin ($n = 15$); or 1:10 000 *Grammostolla spatulata* venom ($n = 20$).

The data are consistent with TRPC1 being a subunit of these SOCs. Resistance to ruthenium red suggests that TRPVs are not involved. These pial arteriolar SOCs are distinct from background channels and SOCs in choroidal arterioles.

Curtis, T.M. & Scholfield, C.N. (2001). *J. Physiol.* **532**, 609–623.

Flemming, R. *et al.* (2002). *J. Physiol.* **543**, 455–464.

Xu, S.Z. & Beech, D.J. (2001). *Circ. Res.* **88**, 84–87.

We thank the BHF for support.

All procedures accord with current UK legislation.

Evidence for expression and function of TRPC channels in rat resistance arteries

A.J. Hill, P.D. Langton and J.M. Hinton

Department of Physiology, University of Bristol, Bristol BS8 1TD, UK

An increase in endothelial cell calcium ($[Ca^{2+}]_i$) is an obligatory precursor to endothelium-dependent relaxations (Nilius & Droogmans, 2001). The principal candidate channels for this influx are the mammalian transient receptor protein (TRP) homologues, the TRPC family. These channels may be stimulated by receptor and/or store-depletion-dependent mechanisms. The contribution of endothelial TRPC channels to relaxation of rat isolated mesenteric artery was investigated using flufenamic acid (FFA) and SKF96365. These compounds are reported to modulate TRPC function (Halaszovich *et al.* 2000; Inoue *et al.* 2001). The expression and localization of these TRPC channels was further investigated using RT-PCR and immunoconfocal microscopy.

Male Wistar rats (200–225 g) were stunned and killed by cervical dislocation. Second-order mesenteric arteries were dissected free, cleaned of connective tissue and mounted in a Mulvany-Halpern wire myograph under normalized tension for isometric recording of force. Arteries were preconstricted with phenylephrine (PE) to 70 % of maximum force (2–5 μM). The application of FFA and SKF96365 to these arteries abolished PE-induced tone in endothelium-intact and endothelium-denuded arteries in a concentration-dependent manner ($n = 7$ and $n = 8$, respectively).

Sequence-specific primers were designed to rat TRPC1–7. Using RNA isolated from whole arterial homogenates the expression of TRPC mRNA was investigated. RT-PCR demonstrated the expression of TRPCs 1, 3 and 6 ($n = 3$). Appropriate positive and negative controls were carried out for each experiment. Immunoconfocal microscopy was used to investigate the localization of TRPC 1, 3 and 6 in fixed arterial sections. TRPC1 and TRPC6 were shown to be expressed in both smooth muscle and endothelial cells. However, expression of TRP3 appeared to be restricted to endothelial cells.

The non-specific effects of FFA and SKF96365 on PE-induced tone demonstrate the unsuitability of wire myography for the study of arterial TRPC channels. Further experiments will investigate the effects of these compounds on Ca^{2+} handling in isolated endothelial cells. Both RT-PCR and immunoconfocal microscopy demonstrate the expression of arterial TRPCs 1, 3 and 6. In conclusion, our data suggest that TRPC1, 3 and 6 are the principal TRPC channels expressed in rat mesenteric arteries. We suggest these channels are candidates involved in $[Ca^{2+}]_i$ influx necessary for endothelium-dependent relaxations.

Halaszovich, C.R. *et al.* (2000). *J. Biol. Chem.* **275**, 37423–37428.

Inoue, R. *et al.* (2001). *Circ. Res.* **88**, 325–332.

Nilius, B. & Droogmans, G. (2001). *Physiol. Rev.* **81**, 1415–1459.

All procedures accord with current UK legislation.

TRPC5 is a glycosylated protein that is expressed and associated with TRPC1 in human blood vessels

S.Z. Xu*, D. McHugh*, F. Zeng*, S. Shah†, C. Munsch†, A. Sivaprasadarao* and D.J. Beech*

**School of Biomedical Sciences, University of Leeds, Leeds LS2 9JT and †General Infirmary at Leeds, Leeds, UK*

TRPCs are calcium-permeable cation channels that respond to calcium-store depletion or receptor-dependent activation of phospholipase C (Montell *et al.* 2002). We have shown that TRPC1 is expressed in a range of blood vessels and is a subunit of store-operated channels in smooth muscle cells of cerebral arterioles (Xu & Beech, 2001). We are now exploring if TRPC1 is associated with other TRPCs in blood vessels. In this study we focused on TRPC5. Male 6- to 8-week-old mice were killed by cervical dislocation according to Schedule 1 procedures. Discarded pieces of human blood vessel were obtained anonymously and with ethical approval from coronary artery bypass operations.

Western blotting was performed on lysates from mouse aorta and the medial layer of human saphenous vein (SV) ($n = 3$). Anti-TRPC1 polyclonal antibody labelled a protein of 90 kDa, close to the predicted mass of 87–93 kDa. Anti-TRPC5 antibodies generated in rabbit or chicken labelled a protein of 140 kDa. In mouse brain lysates, anti-TRPC5 antibody similarly labelled a protein of 140 kDa. After deglycosylation with peptide *N*-glycosidase F ($n = 3$) the protein reduced in size to 110 kDa, very close to the predicted mass of 110–111 kDa. In mouse and human TRPC5 sequences a consensus N-linked glycosylation site is predicted between the third and fourth membrane-spanning segments. Deglycosylation did not have an effect on TRPC1, which lacks a strong consensus N-linked glycosylation site. Vascular smooth muscle cells in sections of human SV and radial artery were stained by anti-TRPC1 and anti-TRPC5 antibodies, with no staining occurring in the presence of pre-immune serum or in the absence of primary antibody. Co-immunoprecipitation studies were performed in the presence of 1 % Triton X-100 on lysates from tsA cells transiently co-expressing FLAG epitope tagged-TRPC1 and TRPC5. Anti-FLAG antibody precipitated TRPC1 and TRPC5, as did anti-TRPC5 antibody ($n = 2$),

confirming the results of Strubing *et al.* (2001). Using polyclonal antibody to TRPC1, similar results were found in lysates of human SV and mouse brain ($n = 2$ for each).

The data suggest that TRPC5 is a glycosylated protein and that it is expressed along with TRPC1 in vascular smooth muscle. We confirm that TRPC1 and TRPC5 co-immunoprecipitate after heterologous expression, and also show their co-association in the medial layer of human vein.

Montell, C. *et al.* (2002). *Cell* **108**, 595–598.

Strubing, C. *et al.* (2001). *Neuron* **29**, 645–655.

Xu, S.Z. & Beech, D.J. (2001). *Circ. Res.* **88**, 84–87.

We thank The Wellcome Trust for support and are grateful to D. Clapham and G. Barritt for rabbit anti-TRPC5 and anti-TRPC1 antibodies, and C. Montell and Y. Mori for TRPC1 and TRPC5 cDNAs.

All procedures accord with current UK legislation.

Altered binding and channel block by dihydropyridines (DHPs) and benzothiazepines (BTZs) in γ1-deficient L-type Ca^{2+} channels from murine skeletal muscle (SM)

B. Held, S. Lehnert and V. Flockerzi

Institut für Pharmakologie & Toxikologie, Universität d. Saarlandes, 66421 Homburg, Germany

The γ1 subunit of the SM L-type Ca^{2+} channel reduces Ca^{2+} influx by reducing the current amplitude and by a negative shift in the steady-state inactivation, whereas the sensitivity to the DHP agonist (−)-Bay K 8644 is not affected (Freise *et al.* 2000). We tested the binding and blocking action of the DHP isradipine and the BTZ diltiazem on the SM L-type Ca^{2+} channel from γ1-deficient and wild-type (WT) mice. The densities of isradipine binding sites were not significantly different at 4 °C (WT: B_{max}, 1.27 ± 0.1 pmol (mg protein)$^{-1}$ (mean ± S.E.M.); K_D, 0.54 ± 0.7 nM, $n = 3$; γ1−/−: B_{max}, 1.26 ± 0.17 pmol (mg protein)$^{-1}$; K_D, 0.54 ± 0.1 nM; $n = 3$). However, at 37 °C binding site densities were significantly reduced in γ1−/− microsomes (γ1−/−: B_{max}, 0.54. ± 0.16 pmol (mg protein)$^{-1}$; $n = 4$; WT: B_{max}, 1.23 ± 0.34 pmol (mg protein)$^{-1}$; $n = 4$). Diltiazem (10 μM) increased isradipine binding site densities to similar levels at 37 °C in WT cells (B_{max}, 2.39. ± 0.55 pmol (mg protein)$^{-1}$; $n = 4$) and γ1−/− cells (B_{max}, 2.02 ± 0.62 pmol (mg protein)$^{-1}$; $n = 4$). This effect was observed in the absence or presence of Ca^{2+}. Apparently, in the absence of γ1 the high-affinity calcium channel blocker binding site within α1S is destabilized at 37 °C; however, binding can be restored in the presence of diltiazem. To test whether the altered binding is reflected in an altered channel sensitivity to these blockers, L-type Ca^{2+} channel currents were measured in myotubes in the whole-cell configuration of the patch-clamp technique as described previously (Freise *et al.* 2000). Ca^{2+} currents (10 mM Ca^{2+} as charge carrier) were activated by step depolarisations from −90 mV to various test potentials in the absence and presence of increasing concentrations of isradipine and diltiazem. The apparent IC_{50} values for Ca^{2+} current inhibition at +20 mV by isradipine and diltiazem were 177 nM and 102 μM (WT cells) and 455 nM and 383 μM (γ1−/− cells), respectively. Accordingly, the current was blocked by 58 % (WT cells) and 38 % (γ1−/− cells) in the presence of 50 nM isradipine and 10 μM diltiazem. The 58 % inhibition observed in WT cells apparently agrees with the 63 % inhibition expected if additive block by isradipine and diltiazem is assumed, whereas in γ1−/− cells, an additive block by only 23 % was expected. Apparently, the block in in γ1−/− cells is more than additive as expected from the binding experiments. From these data, we conclude that the γ1 subunit of the SM L-type Ca^{2+} channel influences the binding and the blocking effects of DHPs and BTZs.

Freise, D. *et al.* (2000). *J. Biol. Chem.* **275**, 14476–14481.

This work was supported by the Deutsche Forschungsgemeinschaft.

All procedures accord with current local guidelines.

Halothane accelerates the onset of ultra slow inactivation in expressed cardiac L-type Ca^{2+} channels

Robert Leach, Amber Rithalia, David Iles*, Mark R. Boyett, Philip M. Hopkins† and Simon M. Harrison

*School of Biomedical Sciences, *School of Biology and †Academic Unit of Anaesthesia, University of Leeds, Leeds LS2 9JT, UK*

A reduction of peak inward L-type Ca^{2+} current (I_{Ca}) as well as acceleration of I_{Ca} inactivation (Pancrazio, 1996) have been implicated in the direct negative inotropic effect of volatile anaesthetics on the heart. Inactivation of I_{Ca} occurs via both Ca^{2+}-dependent and voltage-dependent mechanisms. The latter consists of two kinetically distinct processes, a fast component occurring within milliseconds and an ultra-slow component occurring over seconds (Boyett *et al.* 1994). Using a mammalian heterologous expression system we sought to investigate the effects of halothane on ultra-slow inactivation of L-type Ca^{2+} currents.

HEK293 tsA201 cells were co-transfected with equimolar cDNA encoding cardiac specific isoforms of L-type Ca^{2+} subunits, α_{1C} and β_{2a}, together with green fluorescent protein (GFP). Expression of the α_{1C} subunit was confirmed by immunoblotting of cellular membrane fractions and by immunofluorescent imaging of fixed cells with anti-α_{1C} antibody. Cells were bathed in a Tris-based extracellular solution with 10 mM Ba^{2+} as the charge carrier (to block Ca^{2+}-dependent inactivation). Fluorescent cells were voltage clamped (whole-cell configuration, holding potential −80 mV) and Ba^{2+} currents flowing through L-type Ca^{2+} channels (I_{Ba}) were elicited by 400 ms clamp pulses (from −70 to +60 mV in 10 mV increments) in the absence and presence of 0.6 mM halothane. To investigate the onset of ultra-slow inactivation, cells were clamped from −80 to +10 mV for 20 s during which I_{Ba} continued to inactivate. Experiments were carried out at 22–24 °C; data are expressed as means ± S.E.M. and P values result from paired t tests.

Peak inward I_{Ba} (at +10 mV) was 225 ± 19 pA under control conditions and this was reduced to 89 ± 7 pA by 0.6 mM halothane ($P < 0.001$, $n = 6$). During 20 s pulses, I_{Ba} inactivated with a time constant of 4180 ± 280 ms which was accelerated by 0.6 mM halothane (time constant of 1750 ± 80 ms; $P = 0.02$, $n = 4$). Peak I_{Ba} (during 400 ms pulses from −80 to +10 mV) following a 20 s pulse recovered back to control with a time constant of 3.2 s ($n = 3$) and recovery was slowed by halothane (time constant 7.8 s, $n = 3$). Application of 3.5 mg ml^{-1} pronase to the bath solution to disrupt extracellular domains of the channel reduced the time constant of inactivation. These data suggest that ultra-slow inactivation is a property of α and β channel subunits and that this mechanism appears to involve extracellular domains (as seen in C-type inactivation), which are halothane sensitive.

Boyett, M.R. *et al.* (1994). *Pflügers Arch.* **428**, 39–50.

Pancrazio, J.J. (1996). *J. Physiol.* **494**, 91–103.

This work was supported by The Wellcome Trust.

Identification of a face of the S4 helix that contributes to the stabilisation of the activated state of the *Shaker* potassium channel

D.J.S. Elliott, E.J. Neale, Q. Aziz, T.S. Munsey, M. Hunter and A. Sivaprasadarao

School of Biomedical Sciences, University of Leeds, Leeds LS2 9JT, UK

The *Shaker* voltage-gated potassium channel consists of a central ion conducting pore domain (S5-P-S6) surrounded by a voltage-sensing domain (S1-S4). During depolarisation the voltage-sensing S4 transmembrane segment undergoes a series of motions that lead to opening of the activation gates situated in the pore domain. Here we report the identification of S4 residues that contribute to the stabilisation of the activated state of the channel.

We have previously reported that Cd^{2+} causes a leftward shift in the *G–V* curve and a slowing of deactivation kinetics of *Shaker* channels bearing R365C and R368C mutations (Bannister *et al.* 2000). Here we investigate the effects of Cd^{2+} on cysteine mutants of residues at 356 to 364 of the S4. For this, we expressed mutant channels in *Xenopus* oocytes and measured currents using two-electrode voltage clamp. 100 μM Cd^{2+} caused leftward shifts in the *G–V* curves of the L358C and L361C mutant channels, similar to R365C and R368C. The effect at 100 μM concentration indicates Cd^{2+} co-ordination between the S4 cysteines and another co-ordinating residue. Other mutants were either unaffected or showed rightward shifts.

Further studies on L361C showed that extracellular application of Cd^{2+} caused a slowing of activation kinetics, a leftward shift in the *G–V* curve (-36.2 ± 0.7 mV), and a slowing of the deactivation kinetics (τ_d before and after Cd^{2+} were 0.28 ± 0.02 and 14.86 ± 2.82 s, respectively, means ± S.E.M., $n = 4$). Voltage dependence studies showed that Cd^{2+} may bind to the L361C channels in the closed state but not in the open state.

Effect of Cd^{2+} on a double mutant L361C-R365C was examined. This mutant displayed a leftward shift in its *G–V* curve (-71.7 ± 13.4 mV, $n = 5$) similar to the corresponding single mutants. However, the maximal effects were observed at a Cd^{2+} concentration that is 100-fold lower than that required for the single mutants, indicating a high-affinity binding that may involve both the S4 cysteines and an additional, yet to be identified, liganding residue in the channel.

The leftward shifts and slowing of deactivation kinetics reflect stabilisation of the open state of the channel. Since positions 358 and 361 lie on the same face of S4 as 365 and 368, the present data together with the previous work (Bannister *et al.* 2000) suggest that the face of S4 comprising positions 358, 361, 365 and 368 may contribute to the stabilisation of the activated state of the channel. The question that remains to be addressed is the identification of the residues in the channel with which these residue(s) interact.

Bannister, J.P.A. *et al.* (2000). *J. Physiol.* **525.P**, 67*P*.

The work was supported by The Wellcome Trust.

All procedures accord with current UK legislation.

Evidence for the close proximity of the extracellular ends of the S4 and S5 segments of the *Shaker* potassium channel

E.J. Neale, D.J.S. Elliott, M. Hunter and A. Sivaprasadarao

School of Biomedical Sciences, Worsley Building, University of Leeds, Leeds LS2 9JT, UK

The *Shaker* potassium channel is a member of the six transmembrane family of voltage-gated potassium channels. Consisting of a voltage-sensing domain (S1-S4) and a pore domain (S5-P-S6), these channels form functional tetrameric channels that activate in response to changes in membrane potential. The positively charged S4 segment is believed to move out of the transmembrane field upon depolarisation, but the exact nature of this movement or the mechanism by which it is translated into opening of the pore activation gate is unknown. There is recent evidence that the N-terminal end of S4 moves close to the pore domain during activation (Elinder *et al.* 2001).

Using the Cd^{2+} metal bridge approach, we recently demonstrated (Elliott *et al.* 2002) that four N-terminal residues in S4 (L358, A359, I360 and L361) approach residue E418, just outside S5. This interaction occurs during membrane depolarisation. It has also been demonstrated that S4 residues following L361 do not appear to move close to E418. Here we have examined the two preceding positions (S357 and M356) at the extracellular end of S4 to investigate whether these two residues are also capable of interacting with E418.

Single S4C and double S4C-E418C mutations were introduced into the N-type inactivation-removed Shaker channel. The mutant channels were expressed in *Xenopus* oocytes and potassium currents were recorded using the two-electrode voltage-clamp technique. These currents were compared in the absence and presence of 100 μM extracellular Cd^{2+}, which will form metal bridges between two or more residue side-chains (C, H, M, E or D) if they are approximately 4 Å apart.

The application of Cd^{2+} to the S357C-E418C double mutant but not the corresponding single mutant channels (S357C or E418C) resulted in fast, almost complete loss of conductance ($n = 3$). However, Cd^{2+} slowed the activation kinetics of the S357C single mutant, and the conductance–voltage curve was also shifted by +22 mV. Cd^{2+} had no effect on the M356C-E418C mutant. The Cd^{2+} effect on S357C-E418C was complete even after holding the oocytes at −120 mV during application ($n = 3$).

Since residues S357-L361 form a complete helical turn, the data are consistent with the evidence that S4 rotates during depolarisation. Taken together with our previous data, we propose that residue S357 in the extracellular end of S4 is close to E418 in the extracellular end of S5, in the closed state of the channel, but that during depolarisation the subsequent residues move towards E418.

Elinder, F. *et al.* (2001). *J. Gen. Physiol.* **118**, 1–10.

Elliott, D.J.S. *et al.* (2002). *Pflügers Arch.* **443**, S276.

This work was supported by The Wellcome Trust.

All procedures accord with current UK legislation.

Chronic hypoxia augments the standing outward K^+ current in rat central neurones via an increase in endogenous amyloid β protein levels

L.D. Plant, J.P. Boyle*, Z. Henderson, P.J. Kemp, C. Peers* and H.A. Pearson

*School of Biomedical Sciences and *Institute for Cardiovascular Research, University of Leeds, Leeds LS2 9JT, UK*

The standing outward K^+ current (I_{Kso}) is a major determinant of cerebellar granule neurone (CGN) excitability and is predominantly mediated by an acid-sensitive member of the 2P domain K^+ channel family, TASK (Millar *et al.* 2000). We have recently shown that TASK1 is acutely sensitive to hypoxia in CGN (Plant *et al.* 2002) and so chose to investigate the effects of chronic hypoxia on this physiologically important current.

Primary cultures of rat cerebellar granule neurones were prepared as previously described from tissue obtained from humanely killed animals (Plant *et al.* 2002). For amphotericin B perforated patch-clamp recordings, extracellular and pipette solutions used were those detailed in Plant *et al.* (2001). I_{Kso} was measured in cells by holding at a potential of −20 mV and ramping the voltage to −100 mV at a rate of 100 mV s^{-1}. All values are given as means ± S.E.M.

The effects of chronic hypoxia on I_{Kso} were measured following incubation of cells for 24 h at 2.5 % O_2. Chronic hypoxia significantly increased I_{Kso} measured at −20 mV in CGN from 98 ± 0.1 to 164 ± 1.0 pA pF^{-1} ($n = 34$ and 10, respectively, $P < 0.01$, Student's unpaired t test). This effect could be mimicked by the chronic application of the Alzheimer's disease peptide amyloid β protein (Aβ) to cells. 24 h incubation with 100 nM Aβ elevated I_{Kso} to 170 ± 0.8 pA pF^{-1} ($n = 12$, $P < 0.01$). In both cases (chronic hypoxia and Aβ) the acid-sensitive component of I_{Kso} was increased to a similar extent (82.6 ± 4.0 %, $n = 3$ and 85 ± 4.3 %, $n = 3$, respectively), indicating that both treatments augmented TASK in these cells. To test whether chronic hypoxia was acting via a change in production of endogenous Aβ, cells were exposed to chronic hypoxia and an increase in Aβ was visualised by immunofluoresence. This hypoxia-induced increase in Aβ immunofluoresence could be prevented by incubation with 2-naphthoyl-VF-CHO (γ-IV, 10 μM), an inhibitor of the γ secretase that cleaves amyloid precursor protein to produce Aβ. Crucially, γ-IV also prevented the hypoxia-induced increase in I_{Kso}.

These data indicate that chronic hypoxia upregulates the functional expression of TASK in native neurones. Furthermore, our data indicate that Aβ may represent a key signalling molecule in the modulation of TASK channel activity induced by chronic hypoxia. Such an effect may contribute to the known increased incidence of dementias following hypoxic/ischaemic episodes (Moroney *et al.* 1997).

Millar, J.A. *et al.* (2000). *Proc. Natl Acad. Sci. USA* **97**, 3614–3618.

Moroney, J.T. *et al.* (1997). *Ann. N. Y. Acad. Sci.* **826**, 433–436.

Plant, L.D. *et al.* (2002). *Stroke* (in the Press).

This work was supported by the MRC and The Wellcome Trust.

All procedures accord with current UK legislation.

Hypoxia inhibits the recombinant tandem P domain K^+ channel, hTREK-1, and occludes its activation by arachidonic acid or membrane stretch

P. Miller*, C. Peers†, C.G. Chapman‡, H.J. Meadows‡ and P.J. Kemp*

*Schools of *Biomedical Sciences and †Medicine, University of Leeds, Leeds and ‡GlaxoSmithKline, New Frontiers Park, Harlow, Essex, UK*

Previous studies have suggested that certain native members of the tandem P domain K^+ (K_{2P}) channel family are involved in cellular responses to reduced P_{O_2} (Hartness *et al.* 2001; Plant *et al.* 2002) and that such responses are maintained in recombinant expression systems (Lewis *et al.* 2001). Here, we report the effects of hypoxia on the human recombinant arachidonic acid- and membrane stretch-sensitive K_{2P} channel, hTREK-1 (Meadows *et al.* 2000).

The full-length hTREK-1 was cloned and stably expressed in human embryonic kidney (HEK 293) cells as previously described (Meadows *et al.* 2000). Whole-cell currents were recorded by the patch-clamp technique using solutions and voltage-clamp protocols described by Hartness *et al.* (2001). All data reported herein were taken from currents recorded at a 200 ms test potential of +60 mV from a holding potential of −70 mV. Acute hypoxia (~20 mmHg) was achieved in the recording chamber by perfusing with extracellular solution pre-equilibrated with 100 % N_2.

In normoxia (150 mmHg), K^+ current density was 111 ± 17 pA pF^{-1} (mean ± S.E.M., $n = 10$ cells). Hypoxia caused reversible inhibition of K^+ currents by 38.5 ± 3.7 %, to 68.0 ± 10.7 pA pF^{-1} ($n = 10$, $P < 0.001$, Student's paired t test). Application of arachidonic acid (AA) caused rapid and reversible enhancement of K^+ current density in a concentration-dependent manner, with maximal enhancement (corresponding to a 2.18 ± 0.26-fold increase ($n = 6$, $P < 0.01$) in current density observed when applying 10 μM AA. In the presence of AA (10 μM), exposure to hypoxia reduced K^+ current density to 53.5 ± 17.2 pA pF^{-1} ($n = 6$, $P < 0.01$), a value not significantly different from that seen under hypoxic conditions in the absence of AA. Furthermore, negative pipette pressure of more than 30 mmH_2O significantly increased K^+ current (to 133.2 ± 5.6 % of control; $n = 12$) and this increase was reversed by hypoxia, decreasing currents to 62.5 ± 8.5 % ($n = 4$) of control; a degree of hypoxic K^+ current inhibition normally observed in the absence of membrane stretch.

In conclusion, hTREK-1 is O_2 sensitive when stably expressed in HEK 293 cells. Furthermore, the activation of this channel by either AA or membrane stretch is prevented by hypoxia suggesting that the structural requirements for regulation by fatty acids, stretch and oxygen may co-localise.

Hartness, M.E. *et al.* (2001). *J. Biol. Chem.* **276**, 26499–26508.

Lewis, A. *et al.* (2001). *Biochem. Biophys. Res. Comm.* **285**, 1290–1294.

Meadows, H.J. *et al.* (2000). *Pflügers Arch.* **439**, 714–722.

Plant, L.D. *et al.* (2002). *Stroke* (in the Press).

This work was supported by The Wellcome Trust and the British Heart Foundation.

SUR2A carboxy-terminal domain interaction with Kir6.2 subunits in cloned ATP-sensitive potassium channel channels.

R.D. Rainbow*, M. James†, P.J. Watson†, H. Singh†, I. Ashmole†, D. Lodwick†, N.W. Davies* and R.I. Norman†

*Departments of *Cell Physiology and Pharmacology and †Medicine, University of Leicester, PO Box 138, Leicester LE1 9HN, UK*

Functional ATP-sensitive potassium (K_{ATP}) channels are a hetero-octomer of four inward rectifier Kir6.0 and four sulphonylurea receptor (SUR) subunits. Replacement of the transmembrane domains TMD0, TMD1 or TMD2 in SUR1 with those from multidrug resistance-associated protein 1 impairs assembly and surface expression of K_{ATP} channels (Schwappach, 2000). In this study, possible interactions between the carboxy-terminal domain of SUR2A and Kir6.2 were investigated by co-immunoprecipitation of maltose binding protein (MBP)-tagged SUR2A fragments with Kir6.2 and by analysis of cloned K_{ATP} channel function and distribution in HEK293 cells.

K_{ATP} channel polypeptides were prepared by *in vitro* transcription/translation of cloned cDNA. Two MBP-tagged SUR2A fragments A (amino acids 1254–1545) and B (amino acids 1294–1403) were co-immunoprecipitated with full length Kir6.2 using a polyclonal anti-Kir6.2 antiserum. A third C-terminal domain fragment, C (amino acids 1358–1545) did not co-immunoprecipitate with Kir6.2 under the same conditions, thus indicating a direct interaction between Kir6.2 and a cytoplasmic carboxy-terminal region of SUR2A between residues 1294 and 1358.

HEK293 cells stably expressing full length Kir6.2 and SUR2A were transiently transfected with SUR2A fragments cloned into pIRES2-EGFP. Fractional ATP and glibenclamide-sensitive currents were reduced in inside-out patches from cells transfected with fragments A (0.050 ± 0.004, mean ± S.E.M., $P < 0.001$) and B (0.13 ± 0.02, $P < 0.001$) compared with mock transfected and fragment C (0.93 ± 0.10, $P > 0.05$) transfected cells (control current = 1283 ± 182 pA (S.E.M.), $n = 6$, unpaired *t* test with Bonferroni's multiple comparison test), suggesting a reduced number of functional channels at the cell surface. In mock transfected cells, immunocytochemistry with isoform-specific anti-Kir6.2 and anti-SUR2A antisera revealed a predominant plasma membrane localisation of both subunits. Cell membrane-associated fluorescence was substantially lower and intracellular fluorescence was raised in cells expressing fragments A and B compared with untreated cells or cells expressing fragment C. Thus SUR2A fragments containing residues 1294–1358 reduce current by decreasing channel subunits in the cell membrane.

We have identified a site in the carboxy-terminal domain of SUR2A, between residues 1294 and 1358, whose direct interaction with full length Kir6.2 is crucial for assembly of functional K_{ATP} channels.

Schwappach, B. *et al.* (2000). *Neuron* **26**, 155–167.

This work was funded by the BHF and MRC. We thank A. Tinker for Kir6.2/SUR2A cell lines.

In vitro recovery of ATP-sensitive potassium channels in β-cells from patients with hyperinsulinism in infancy; effects of low temperature and BPDZ 154

Karen E. Cosgrove*, Ana-Maria Gonzalez*, Anne T. Lee*, Philippa Barnes*, Khalid Hussain†, Al Aynsley-Green†, Keith J. Lindley†, Bernard Pirotte‡, Philippe Lebrun§ and Mark J. Dunne*

**Biomedical Science, Sheffield University, Sheffield, UK, †Institute of Child Health, London, UK, ‡Department of Medicinal Chemistry, University of Liège, Liège, Belgium and §Laboratory of Pharmacology, Free University of Brussels, Brussels, Belgium*

Hyperinsulinism in infancy (HI) is the most common cause of recurrent or persistent hypoglycaemia in early childhood. The disease is principally caused by defects in the ATP-sensitive K channel (K_{ATP}) genes ABCC8 (SUR1) and KCNJ11 (Kir6.2), which can result in altered nucleotide regulation, channel gating, subunit assembly or subunit trafficking. Loss of K_{ATP} channels causes inappropriate Ca^{2+} channel activity and uncontrolled insulin release as a consequence. In this study we have investigated the cell surface expression of functional K_{ATP} channels in β-cells isolated from patients with HI by maintaining isolated cells under a variety of controlled conditions designed to modulate post-translational events associated with the trafficking of membrane proteins. Insulin-secreting cells were isolated from two patients with diffuse HI. Patients N79 and N94 were unrelated, and failed to respond adequately to diazoxide and/or Sandostatin or Octreotide *in vivo*. As a result both patients required a subtotal pancreatectomy to control hypoglycaemia.

Following surgery (with informed consent and Local Ethics Committee approval), a controlled collagenase digestion procedure was used to isolate intact islets of Langerhans, and single β-cells were liberated by mechanical agitation in a standard Ca-free extracellular solution. Single cells were subsequently maintained under standard tissue culture conditions at 37 °C or at either 37 or 25 °C in the presence or absence of: (1) 10 nM phorbol myristate acetate (PMA), 2 μM forskolin and 100 μM 3-isobutyl-1-methylxanthine (IBMX); (2) 2.5 mM 4-phenylbutryate; or (3) the K_{ATP} channel agonist 10 μM BPDZ 154, for up to 40 h. The surface expression of functional K_{ATP} channels was assessed by patch-clamp methods using isolated patches of cell membrane. RNA was extracted from isolated tissue using standard protocols and RT-PCR performed to document the expression of K_{ATP} channel mRNAs using specific oligonucleotide primers directed against SUR1 and Kir6.2. In N79 β-cells maintained at 37 °C, limited K_{ATP} channel activity was seen in only 38 % of cells ($n = 3/8$) as a consequence of defects in the C-terminal region of SUR1 (oligonucleotide primers to Kir6.2 and all three regions of SUR1 generated PCR products in control cells, whilst in N79 only Kir6.2 and the N-terminal region of SUR1 were amplified). By contrast when N79 β-cells were maintained at 25 °C (either with or without exposure to 2.5 mM 4-phenylbutyrate), 73 % of cells ($n = 8/11$) expressed functional channels that responded to ADP (0.5 mM) and diazoxide (0.5 mM). Maintenance of N79 β-cells at 37 °C in the presence of 100 μM IBMX, 10 nM PMA and 2 μM forskolin did not enhance expression of functional K_{ATP} channels ($n = 3$). Under standard cell culture conditions at 37 °C, there were no operational K_{ATP} channels in N94 β-cells, $n = 6$. However, when cells were maintained at 37 °C in tissue culture media supplemented with either IBMX, PMA and forskolin or 10 μM BPDZ 154, this led to a recovery of K_{ATP} channel currents that were inhibited by ATP, $n = 4/10$ cells.

These data document that modulation of post-translational events can potentially lead to the recovery of endogenous K_{ATP} channel function in HI β-cells.

All procedures accord with current local guidelines.

Glucose induces acute changes in the expression of ATP-sensitive potassium channels in the pancreatic β-cell line INS-1

A.J. Smith, C.J. Partridge, L.A. Mair and A. Sivaprasadarao

School of Biomedical Sciences, University of Leeds, Leeds LS2 9JT, UK

ATP-sensitive potassium (K_{ATP}) channels of the pancreas play a key role in the regulation of glucose-stimulated insulin secretion (GSIS). They couple the metabolic activity to membrane excitability, preventing insulin secretion when the metabolic state of the cell is low. Although glucose regulation of K_{ATP} channel function has been well characterised, it is not known whether the metabolic state of the cell has any influence on regulation of channel density within the cell.

To address this, changes in K_{ATP} channel density were examined in the GSIS responsive INS-1 β-cell line. K_{ATP} channels were visualised using antibodies raised against each of the two channel subunits SUR1 and Kir6.2 then viewed by confocal microscopy. Cells grown in 3 mM glucose showed much higher K_{ATP} channel density compared with those in 25 mM glucose. By contrast, cells grown overnight in 25 mM glucose showed reduced expression, but when returned to 3 mM glucose there was rapid increase in K_{ATP} channel expression. Cells previously incubated in 3 mM glucose when grown in 25 mM showed little change in K_{ATP} expression. The level of K_{ATP} expression was also seen to be dependent on glucose concentration. At hypoglycaemic and normal physiological glucose (2–5 mM) K_{ATP} channel expression is high, whereas in hyperglycaemic glucose (> 11 mM) K_{ATP} channel expression is decreased.

Low glucose levels stimulate an increase in the expression of the K_{ATP} channel subunits SUR1 and Kir6.2. To study the rate of K_{ATP} induction we used [^{35}S]-methionine pulse chase analysis. Cell lysates were collected, subjected to immunoprecipitation with anti-SUR1 antibody and proteins subjected to SDS-PAGE/autoradiography. Bands of ~260 and ~175 kDa correspond to the expected sizes of mature (glycosylated) and immature forms of SUR1, respectively. In addition, a 44 kDa band corresponding to the size of Kir6.2 was co-immunoprecipitated. Expression of both the mature SUR1 and Kir6.2 increased in parallel, inducing an increase in the channel density of the functional channel ($n = 3$).

The fact that the increase occurs within minutes of lowering glucose indicates that the change in channel density is likely to have an important physiological role in GSIS. One possibility is that the increased channel numbers together with the increased activity of the channel may help to rapidly terminate insulin secretion and thus protect the animal from any danger of severe hypoglycaemia.

This work was supported by the MRC and the Emma and Leslie Reid Scholarship.

Effects of *in vitro* chronic hypoxia on K^+ currents in isolated human internal mammary artery smooth muscle cells

P. Kang*, K.E. Porter*, P.J. Kemp† and C. Peers*

**Institute for Cardiovascular Research and †School of Biomedical Sciences, University of Leeds, Leeds LS2 9JT, UK*

Altered ion channel expression in response to prolonged hypoxia has been demonstrated in different cell types (e.g. Smirnov *et al.* 1994; Green & Peers, 2001), and probably contributes to remodelling of overall tissue responses to such insults. Here, we describe a preparation designed to examine the effects of chronic hypoxia on K^+ channel expression in smooth muscle cells isolated from human internal mammary artery (IMA).

IMA samples were collected from patients undergoing coronary bypass grafting with local ethical permission, cleaned of adventitia, opened longitudinally and cut into segments *ca* 3–5 mm in length. These were then pinned, lumen uppermost onto Sylgard®-coated 60 mm Petri dishes using A1 Minuten pins, and immersed in RPMI culture medium supplemented with 30% fetal calf serum. Tissues were cultured at 37°C in humidified incubators gassed with either air and 5% CO_2, or a gas mixture of 2.5% O_2, 87.5% N_2 and 5% CO_2. After 18 h, smooth muscle cells were dispersed as described previously (Kamishima *et al.* 2000), and allowed to adhere to poly-L-lysine-coated coverslips. Whole-cell patch-clamp recordings were made using pipette and extracellular solutions as previously described (Peers & Carpenter, 1998). Currents were evoked by step depolarizations (100 ms, 0.2 Hz) up to +60 mV from a holding potential of −70 mV.

Cell capacitance was significantly smaller ($P < 0.05$, Student's unpaired t test) in normoxically cultured cells at 12.4 ± 1.1 pF (mean ± S.E.M., $n = 14$ cells from 8 patients) compared with 15.9 ± 1.3 pF in hypoxic cells (12 cells from the same 8 patients). K^+ currents typically activated at *ca* −20 mV and increased in amplitude with increasing depolarization. Current density was significantly greater ($P < 0.05$, ANOVA) in cells cultured normoxically, compared with those maintained under hypoxic conditions. For example, at a test potential of +60 mV, current density was 55.3 ± 17.4 pA pF^{-1} in control cells, and 21.8 ± 5.8 pA pF^{-1} in hypoxic cells.

Our results indicate that this preparation allows isolation of viable smooth muscle cells from human tissue maintained *in vitro* for up to 48 h. Our preliminary results also suggest that K^+ channel expression is sensitive to changes in O_2 levels *in vitro*.

Green, K.N. & Peers, C. (2001). *J. Neurochem.* **77**, 953–956.

Kamishima, T. *et al.* (2000). *J. Physiol.* **522**, 285–295.

Peers, C. & Carpenter, E. (1998). *J. Physiol.* **512**, 743–750.

Smirnov, S.V. *et al.* (1994). *Am. J. Physiol.* **266**, H365–370.

This work was supported by the British Heart Foundation, The Wellcome Trust and Pfizer Central Research.

All procedures accord with current local guidelines and the Declaration of Helsinki.

Reversal of chronic hypoxia-induced alteration in K_{Ca} channels in pulmonary artery smooth muscle cells upon air breathing

Sébastien Bonnet*, Eric Dubuis†, Christophe Vandier† and Jean-Pierre Savineau*

**EMI INSERM* (*9937*), *University Bordeaux 2, France and* †*LABPART, University Tours, France*

Chronic hypoxia (CH)-induced pulmonary artery hypertension is accompanied by functional changes in pulmonary arteries. Some of these changes are reversed by returning animals to normoxic environment (Bonnet *et al.* 2002).

In the present work, we investigated the reversal of CH-induced alteration on Ca^{2+}-activated K^+ channels (K_{Ca}) of rat pulmonary artery smooth muscle cells (PASMC) upon air breathing. Rats were exposed to a hypobaric environment (50.5 kPa) for 3 weeks (CH rats) and then subjected to a normoxic environment for 3 weeks (normoxia-recovery rats (Rec)) and compared with rats maintained in a normoxic environment (control rats). Animals were terminally anaesthetized with pentobarbital sodium (60 mg kg^{-1} I.P.). Experiments were performed in freshly enzymatically isolated PASMC using the patch-clamp technique to record macroscopic and unitary iberiotoxin (IbTx)-sensitive K^+ currents (K_{Ca}).

The current density of K_{Ca} was reduced in CH PASMC but were increased (2.2 times) in recovery PASMC in comparison with the control PASMC. The resulting current–voltage relationship indicated no significant difference in the single-channel conductance which was 228, 234 and 238 pS, respectively, in control, CH and Rec groups. NP_o values were fitted by a Boltzmann function ($NP_o = NP_{max}/(1 + \exp(V - V_{½})/k)$ with N the number of channels in the patch, P_o the open state probability, $V_{½}$ the voltage for half-maximal activation and k the slope factor (which is an indicator of the single-channel voltage sensitivity), indicating that the k value was not altered. In contrast, $V_{½}$ was significantly different ($P < 0.05$, ANOVA, *post-hoc t* test) in PASMC from CH and normoxia-recovery rats compared with control for all $[Ca^{2+}]_i$ studied (Table 1).

Table 1. The effect of chronic hypoxia (CH) and normoxia-recovery on $V_{½}$ values for three different $[Ca^{2+}]_i$

	$[Ca^{2+}]_i$ 10 nM	$[Ca^{2+}]_i$ 100 nM	$[Ca^{2+}]_i$ 1000 nM
Control	110.4 ± 3.6 ($n = 4$)	72.9 ± 2.47 ($n = 5$)	50.1 ± 2.1 ($n = 5$)
CH	113.3 ± 6.4 ($n = 5$)	87.5 ± 3* ($n = 6$)	67.1 ± 2.1* ($n = 6$)
Recovery	93 ± 3.18*# ($n = 6$)	51.8 ± 1.6*# ($n = 5$)	26.9 ± 4.18*# ($n = 5$)

Data are means ± S.E.M. *$P < 0.05$ compared with control; *#$P < 0.05$ compared with both control and CH.

All these results demonstrate that chronic hypoxia and then recovery upon air breathing modulate K_{Ca} currents, probably and respectively, by a decrease and an increase of calcium sensitivity of K_{Ca} channels.

Bonnet, S. *et al.* (2002). *Cardiovasc. Res.* **53**, 1019–1028.

All procedures accord with current National and local guidelines.

Effects of severe hypoxia on inward rectifying potassium current in ventricular myocytes of crucian carp (*Carassius carassius*) heart

Vesa Paajanen and Matti Vornanen

University of Joensuu, Department of Biology, PO Box 111, 8010 Joensuu, Finland

Some ectothermic vertebrates are especially tolerant to anoxia and it is has been hypothesized that this requires a decrease in the number or the activity of ion channels in order to reduce energy consumption by ATP-dependent ion pumping (channel arrest hypothesis). Several studies have provided indirect evidence in favour of the channel arrest hypothesis; however, only a limited number of experiments have examined the activity of ion channels directly from animals exposed to long-term hypoxia or anoxia *in vivo*.

Using the whole-cell and cell-attach single-channel patch-clamp methods, we compared the inward rectifying K^+ current (I_{K1}), which is the primary current affecting resting membrane potential, in isolated cardiac myocytes of normoxic and hypoxic crucian carp, an anoxia-tolerant fish. Crucian carp ($N = 68$) were kept in large aerated tanks (control) or in 2 l Erlenmeyer bottles from which oxygen was removed with N_2 gassing (hypoxic). The duration of hypoxia varied from 4 to 28 days. Electrophysiological experiments were made with freshly isolated ventricular myocytes at the acclimation temperature (5°C) of the fish (fish were humanely killed). All experiments were conducted with the permission of the local committee for animal experimentation and comply with the guidelines of animal experimentation in Finland.

Severe hypoxia (< 0.4 g l^{-1} O_2) from 4 days to 28 days in duration did not have any effect on I_{K1}. Whole-cell conductance of I_{K1} was 0.6 ± 0.05 nS pF^{-1} (mean ± S.E.M.) in normoxic fish and did not change during the 4-week hypoxic period (cells isolated every fourth day; $n = 17$ or 18). Over the same time period Na^+–K^+-ATPase activity decreased 33 % ($P < 0.03$, unpaired *t* test; $n = 8$). Single-channel conductance was unchanged by hypoxia, being 20.5 ± 0.8 pS ($n = 17$) in control fish and 21.4 ± 1.1 pS ($n = 11$) in hypoxic fish when symmetric 140 mM K^+ solutions were used. Furthermore, the open probability of the channel was unchanged being 0.80 ± 0.03 and 0.74 ± 0.04 in control and hypoxic fish, respectively ($n = 18$). Additionally open and closed times had identical distributions in normoxic and hypoxic fish.

These results suggest that the inward rectifier K^+ channels are not modified by severe hypoxia in ventricular cardiac myocytes of the crucian carp. We conclude that crucian carp cardiac myocytes obtain energy savings through 'spike arrest' due to hypoxic bradycardia rather than via channel arrest.

This study was supported by the Academy of Finland (project #53481).

All procedures accord with current National guidelines.

Acclimation to cold increases the density of the delayed rectifier K^+ current (I_{Kr}) in rainbow trout atrial myocytes

Matti Vornanen

Department of Biology, University of Joensuu, PO Box 111, 80101 Joensuu, Finland

Ectothermic animals inhabiting cold environments require physiological compensation mechanisms to maintain a short

enough cardiac action potential (AP) duration to allow adequate heart rates and fast contraction kinetics in the cold. To understand the significance of I_{Kr} in physiological cold adaptation of the ectothermic heart, the density and kinetics of the E-4031-sensitive (1 μM) current (I_{Kr}) was measured in atrial myocytes of rainbow trout (*Oncorhynchus mykiss*). The fish were reared for a minimum of 4 weeks either at 18 °C (warm-acclimated, WA) or 4 °C (cold-acclimated, CA) and atrial myocytes were isolated by enzymatic digestion. Experiments were conducted at the acclimation temperature of the animals (either 4 or 18 °C) and at 11 °C. All experiments were done with the permission of the local committee for animal experimentation and comply with the current legislation in Finland. The animals were humanely killed at the end of the experiments.

Instantaneous current–voltage relationships of I_{Kr} were linear and current densities were 12.7 ± 1.3 (mean ± S.E.M., $n = 7$; 4 °C) and 13.1 ± 2.9 pA pF^{-1} ($n = 6$; 18 °C) ($P > 0.05$, Student's unpaired t test) at 0 mV for CA and WA trout, respectively. This indicates an almost perfect thermal compensation of current amplitude. At 11°C, the current density was 28.3 ± 2.7 ($n = 7$) and 9.2 ± 1.5 pA pF^{-1} ($n = 6$) ($P < 0.001$) for CA and WA trout, respectively, suggesting that the expression of I_{Kr} is strongly enhanced by cold adaptation. Deactivation and inactivation kinetics of I_{Kr} were strongly temperature dependent and identical for atrial myocytes of CA and WA rainbow trout, suggesting that thermal acclimation does not modify channel gating (Fig. 1). Due to the temperature dependence of current kinetics, acute temperature changes are expected to modify the duration of the AP through changes in I_{Kr}.

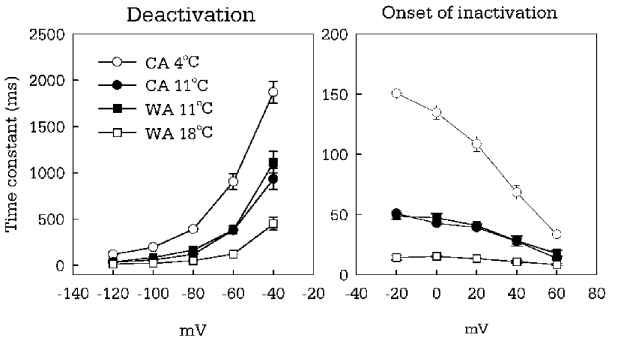

Figure 1. Temperature and voltage dependence of deactivation and inactivation kinetics of I_{Kr} in atrial myocytes of CA and WA rainbow trout. The results are means ± S.E.M. from 5–9 myocytes.

Voltage-clamp experiments using physiological APs as the command waveform indicated that, due to incomplete deactivation, an accumulation of I_{Kr} occurs at physiological pacing rates (30 b.p.m.) in atrial myocytes of the CA trout at 4 °C and generates a strong repolarising current immediately at the onset of the AP. In WA trout at 18 °C, I_{Kr} develops more slowly during the AP.

In summary, the present results show that the expression of I_{Kr} is regulated in a temperature-dependent manner in atrial myocytes of the trout heart, and that the high density of I_{Kr} and the rate-dependent accumulation of I_{Kr} in CA fish probably underlie the maintenance of the short duration AP required for adequate cardiac function in a cold environment.

This study was supported by the Academy of Finland (project #53481).

All procedures accord with current National and local guidelines.

Location and accessibility to thimerosal of residue C160 of the Kir2.3 potassium channel

M. Ju and D. Wray

Biomedical Sciences, University of Leeds, Leeds LS2 9JT, UK

The Kir2.3 potassium channel possesses cysteines at extracellular and intracellular positions where cysteine-binding reagents, such as thimerosal, are known to act (Bannister *et al.* 1999). Additionally it possesses a cysteine half-way down the pore-lining M2 region at position C160, although it is not known if this residue is accessible to extracellularly applied thimerosal. The object of this work was to investigate the accessibility to thimerosal of this residue.

Extracellularly applied thimerosal is already known to act on extracellularly facing cysteines C79 and C140, so that experiments were carried out in the background of the channel C79S/C140S. Mutations were made using the PCR Quickchange method, and the further mutation C160S was made. RNA for these mutants and wild-type Kir2.3 was injected into *Xenopus* oocytes and two-electrode voltage-clamp recordings were made 1–2 days later at room temperature. Hyperpolarising pulses were applied at 0.1 Hz from a holding potential of 0 mV. The effects of bath-applied thimerosal (100 μM) were obtained by perfusing continuously during repetitive pulses to −100 mV.

The current kinetics and I–V curves for the mutants were very similar to those of wild-type. Thimerosal induced an inhibition of the currents for the wild-type and all the mutants, but the extent of inhibition differed. The extent of inhibition by thimerosal of the triple mutant C79S/C140S/C160S (by 43.7 ± 2.0 %, $n = 6$, mean ± S.E.M.) was significantly ($P < 0.05$, Student's unpaired t test) less than the inhibition of the double mutant C79S/C140S (by 84.5 ± 4.3 %, $n = 5$) or the wild-type channel (by 88.7 ± 3.2 %, $n = 6$). By comparing experiments where thimerosal was applied for 5 min in the presence or absence of stimulation, the effects of thimerosal were similar whether for wild-type or mutants, indicating lack of use-dependent effect of thimerosal. Furthermore, the inhibition induced by thimerosal was irreversible by washing for 5 min, but was reversed by the application of the reducing agent dithiothreitol, confirming that the effects occurred via covalent modification.

The results show that extracellularly applied thimerosal can reach residue C160 and produce inhibition. This M2 residue is therefore pore-facing and probably lies in an intracellular-facing large cavity, as also occurs for the corresponding residue in Kv2.1 (Lu *et al.* 2001) and in Kv6.2 (Loussouarn *et al.* 2000). Thimerosal is membrane permeable, and probably reaches this residue by first crossing the membrane and entering the cavity from the intracellular side.

Bannister, J. *et al.* (1999). *Pflügers Arch.* **438**, 868–878.

Loussouarn, G. *et al.* (2000). *J. Biol. Chem.* **275**, 1137–1144.

Lu, T. *et al.* (2001). *J. Gen. Physiol.* **118**, 509–521.

All procedures accord with current UK legislation.

Interaction between inwardly rectifying potassium channel, Kir 2.1, and synapse-associated protein-97 in the porcine coronary artery

L.J. Sampson*, C. Dart† and M.L. Leyland*

*Departments of *Biochemistry and †Cell Physiology and Pharmacology, University of Leicester, University Road, Leicester LE1 7RH, UK*

Inwardly rectifying potassium channel, Kir 2.1, plays an important role in the control of membrane excitability in the vasculature (Quayle *et al.* 1997). Synapse-associated protein-97 (SAP97) belongs to a group of membrane-associated guanylate kinase proteins (MAGUKs) that interact with potassium channels through specialised PDZ domains. The inwardly rectifying potassium channel, Kir 2.2, carries a C-terminal PDZ binding motif and co-localises with SAP97 in ventricular myocytes (Leonoudakis *et al.* 2001). The present study examined the interaction of SAP97 with Kir 2.1 in the porcine coronary artery. Expression of inwardly rectifying channels belonging to the Kir 2.0 family and SAP97 in the porcine coronary artery was examined by RT-PCR. Whole hearts of adult pigs were obtained from a local abattoir, coronary arteries dissected and total RNA extracted. Sequence-specific oligonucleotide primers were designed against Kir 2.1, Kir 2.2, Kir 2.3, Kir 2.4 and SAP97. A one-tube RT-PCR reaction was performed and transcripts for Kir 2.1 and SAP97 detected. RT-PCR failed to detect transcripts for Kir 2.2, 2.3 and 2.4 ($n = 3$).

Association of SAP97 with the C-terminal PDZ binding motif of Kir 2.1 (amino acids 424–428) was examined using GST pull-down assays. A GST-tagged peptide representing C-terminal amino acids (421–428) of Kir 2.1 isolated SAP97 from porcine coronary artery lysates and HEK-293 cells transfected with cDNA for SAP97, a kind gift from Dr C. Garner (University of Birmingham, Alabama, USA). GST alone failed to bind SAP97 ($n = 3$).

SAP97 harbours three distinct PDZ domains (PDZ 1–3). Interaction of individual domains with Kir 2.1 was defined by overlay assay. A His-tagged construct representing C terminal amino acids of Kir 2.1 (307–428) was overlaid with GST-tagged fusion proteins representing single PDZ domains of SAP97. The C terminus of Kir 2.1 interacted specifically with PDZ domains 2 and 3 of SAP97. PDZ domain 1 failed to interact.

These data demonstrate that the inwardly rectifying potassium channel, Kir 2.1, and MAGUK protein, SAP97, are expressed in porcine coronary artery. Furthermore, Kir 2.1 interacts with PDZ domains 2 and 3 of SAP97, present in porcine coronary artery, via its C terminal PDZ binding motif.

Leonoudakis, D. *et al.* (2001). *J. Cell Sci.* **114**, 987–998.

Quayle, J.M. *et al.* (1997). *Physiol. Rev.* **77**, 1165–1232 .

This work was supported by the British Heart Foundation.

Activation kinetics of rat and human Kv2.1 potassium channels: a C terminal determinant

L. Rashleigh, M. Ju, E. Leadbitter and D. Wray

Biomedical Sciences, University of Leeds, Leeds LS2 9JT, UK

The human and rat forms of the Kv2.1 potassium channel have identical amino acids over the membrane-spanning regions, but differ only in the N- and C-terminal domains (Frech *et al.* 1989; Albrecht *et al.* 1993). Despite this high degree of similarity, the activation rate of rat Kv2.1 is much faster than for the human channel. We have already demonstrated that N terminal residues play a role in activation kinetics (Ormond *et al.* 2001). In the C-terminal region, there are 49 amino acids that are different between the two channels, and here we have investigated a possible role of C-terminal residues in determining activation kinetics.

For this, cDNA chimaeras were made between rat and human forms of the Kv2.1 channel. These were constructed either by cutting with restriction enzymes and subsequent ligation of fragments, or by using the overlap extension PCR method. cRNAs for these chimaeras and for the wild-type channels were injected into *Xenopus* oocytes, and voltage-clamp recordings were made 1–2 days later at room temperature. Depolarizing pulses were applied at 0.1 Hz from a holding potential of −80 mV, and activation times were measured from 10 to 90 % maximal current.

The first chimaera with amino acids 108–740 of the rat channel replaced by the corresponding human channel showed an activation time (46 ± 4 ms at 0 mV, $n = 4$, mean ± S.E.M.) that was not significantly different (Student's unpaired t test) from that for wild-type rat channel (48 ± 6 ms, $n = 10$). This indicates that amino acids 108–740 are not likely to play a part in activation kinetics. On the other hand, a second chimaera with amino acids 596–853 of the rat channel replaced by human sequence displayed a significantly ($P < 0.05$) longer activation time (92 ± 20 ms, $n = 9$) than that for the rat channel (42 ± 15 ms, $n = 5$), and in fact was similar to the activation time for human wild-type channel. The results for these two chimaeras therefore suggest that amino acids 741–853 probably contain a domain that plays a role in activation kinetics. A third chimaera was made to further define this domain, with amino acids 741–796 of the rat channel replaced by the corresponding human sequence. For this chimaera, the activation time (62 ± 8 ms, $n = 6$) was not significantly different from that for rat wild-type (54 ± 15 ms, $n = 5$). Taken together, these results indicate that a region spanning amino acids 797–853 of the C-terminal region contains a domain that plays a role in determining the activation kinetics of the Kv2.1 channel.

Albrecht, B. *et al.* (1993). *Receptors and Channels* **1**, 99–110.

Frech, G.C. *et al.* (1989). *Nature* **340**, 642–645.

Ormond, S. *et al.* (2001). *J. Physiol.* **535.P**, 6*P*.

All procedures accord with current UK legislation.

Actions of the selective serotonin re-uptake inhibitor fluvoxamine on HERG-mediated potassium current in a mammalian cell line

James T. Milnes, Jules C. Hancox and Harry J. Witchel

Department of Physiology and Cardiovascular Research Laboratories, University of Bristol, School of Medical Sciences, University Walk, Bristol BS8 1TD, UK

Selective serotonin re-uptake inhibitors (SSRIs) are generally considered to compare favourably with tricyclic antidepressants in terms of their cardiac safety profile. Fluvoxamine is a SSRI that can be associated at excessively high concentrations with QT interval prolongation (Rodriguez *et al.* 1999) and arrhythmia (Manet *et al.* 1993). Excessive ventricular action potential prolongation can lead to the acquired long QT syndrome and to the polymorphic ventricular tachyarrhythmia *torsade de pointes* (Viskin, 1999). I_{Kr} and the current carried by its cloned

equivalent HERG mediate an important repolarizing current, which when blocked by a wide variety of clinically used drugs leads to ventricular action potential prolongation and its associated risks. The objectives of this study were first to determine whether or not fluvoxamine can inhibit K^+ channels encoded by HERG and, second, to characterize the nature of any observed effect.

Heterologous HERG K^+ current (I_{HERG}) was measured at 37 °C in a mammalian cell line (HEK 293) stably expressing HERG channels, using the whole-cell patch-clamp technique. Cells were superfused with a physiological (Na^+-based) Tyrode solution, and the pipette solution was a K^+-based intracellular salt solution. I_{HERG} was sensitive to blockade by fluvoxamine. A total of six different concentrations of fluvoxamine between 10 nM and 30 μM were tested using a minimum of six replicates for each concentration. When the holding potential was −80 mV I_{HERG} 'tails' at −40 mV following an activating pulse to +20 mV were blocked with a half-maximal inhibitory concentration (IC_{50}) of 3.63 μM (95 % CI: 2.92–4.5 μM) and a Hill coefficient of 0.75 (95 % CI: 0.62–0.89). The inhibition of I_{HERG} during applied test pulses and of I_{HERG} 'tails' by fluvoxamine was observed to be voltage dependent. Fluvoxamine exerted a dual effect, with current at more negative test pulses being increased in the presence of drug, whilst at −10 mV and more positive to this blockade became evident. These observations corresponded with a significant ~−10 mV ($P < 0.001$, paired t test, $n = 7$) shift in the voltage-dependent activation curve for I_{HERG}.

The results demonstrate that fluvoxamine can inhibit I_{HERG} within a clinically relevant concentration range. Thus observed alterations to the electrocardiogram and arrhythmia at excessively high fluvoxamine concentrations may in part be due to the drug's ability to block HERG K^+ channels.

Manet, P. *et al.* (1993). *Therapie* **48**, 62–63.

Rodriguez, D.L.T. *et al.* (1999). *Ther. Drug Monit.* **23**, 435–440.

Viskin, S. (1999). *Lancet* **354**, 1625–1633.

This work was supported by the British Heart Foundation.

All procedures accord with current UK legislation.

Structural determinants of HERG potassium channel block by ibutilide and clofilium

M. Perry*, M. Degroot†, R. Helliwell†, D. Leishman† and J. Mitcheson*

**Department of Cell Physiology and Pharmacology, University of Leicester, Leicester and †Ion Channel Group, Pfizer Global Research and Development, Sandwich*

Block of human *ether-a-go-go*-related gene (HERG) K^+ channels by a variety of medications has been linked to acquired long QT syndrome, a disorder of cardiac repolarisation that predisposes to lethal arrhythmias. Methanesulfonanilide compounds, such as ibutilide, dofetilide and MK499, are potent open channel blockers of HERG. Recently, we identified residues in the inner cavity of HERG, which form the binding site for MK499 (Mitcheson *et al.* 2000). Two aromatic residues (Y652 and F656) are particularly important structural determinants of drug block for all compounds tested so far, and all have multiple aromatic groups. To determine if multiple aromatic groups were necessary for interactions with Y652 and F656, we investigated the binding sites of clofilium and ibutilide, which each have a long aliphatic chain but only a single aromatic group. In addition, whereas ibutilide has a methanesulfonanilide moiety, clofilium does not, allowing us to investigate the importance of this chemical group.

The two-microelectrode voltage-clamp technique was used to record membrane currents in isolated *Xenopus* oocytes injected with cRNA. The sensitivity to block by clofilium and ibutilide was investigated in channels in which individual residues in the pore helix (T623 to V625) and S6 (L646 to Y667), predicted to line the inner cavity, had been mutated to alanine. Oocytes were repetitively depolarised from −90 to 0 mV for 5 s, and tail currents elicited by steps to −70 mV. Both ibutilide and clofilium were used at a concentration of 300 nM ($10 \times IC_{50}$), both of which blocked WT HERG to ~20 % of control current. Data are presented as means ± S.E.M.

In most cases mutating residues to alanine had little effect on drug block. However, seven mutants (T623A, S624A, V625A, G648A, Y652A, F656A and V659A) were profoundly insensitive to ibutilide, with 75 to 100 % ($n \geqslant 6$) of current remaining after drug block. Similar results were obtained for clofilium, apart from two mutants within the pore region, T623A and V625A, which were more sensitive to clofilium (60 ± 4 and 69 ± 6 % of control current after drug block, respectively).

These data suggest that seven residues are involved in binding of ibutilide and clofilium. Since mutations of both Y652 and F656 residues, which were previously thought to interact with aromatic groups on the drugs, produce channels which are insensitive to both ibutilide and clofilium, it seems likely that these aromatic residues can interact with both aliphatic and aromatic groups. In addition, the greater sensitivity of the pore helix mutants to clofilium, when compared with ibutilide, suggests that this region may be important for interacting with the methanesulfonanilide moiety.

Mitcheson, J. *et al.* (2000). *PNAS* **97**, 12329–12333.

This work was supported by Pfizer Global Research and Development.

All procedures accord with current UK legislation.